Mon. Not. R. Astron. Soc. **000**, 000–000 (0000) Printed 1 February 2008 (MN LATEX style file v1.4)

# High-redshift radio galaxies and quasars at sub-millimetre wavelengths: assessing their evolutionary status.

D. H. Hughes[1,2], J. S. Dunlop[1] & S. Rawlings[2]

1. *Institute for Astronomy, Dept. of Physics & Astronomy, University of Edinburgh, Royal Observatory, Edinburgh, EH9 3HJ, U.K.*
2. *Astrophysics, Nuclear Physics Laboratory, Oxford University, Keble Rd., Oxford OX1 3RH, U.K.*



**ABSTRACT**

We present new results of a study of the sub-millimetre continuum emission from a sample of 9 radio galaxies and 4 radio-quiet quasars at redshifts $z = 0.75 - 4.26$. The observations were made at $800\mu m$, using the single-element bolometer UKT14 on the James Clerk Maxwell Telescope (JCMT), reaching a typical r.m.s. sensitivity of $\sigma_{rms} \sim 4\,$mJy and represent some of the deepest submillimetre extragalactic measurements made to date. Three detections were achieved, of which two are secure (4C41.17, Dunlop *et al.* (1994) and H1413+117) and one (53W002) is tentative, whilst comparable upper-limits were obtained for 7 of the 10 remaining sources. We use these data as the motivation for a detailed discussion of the conversion from submillimetre and millimetre continuum fluxes to dust/gas masses and star formation rates at high-redshift, and determine these quantities from our own and other data on high-redshift radio-galaxies and quasars. In particular we have investigated the impact of the four main sources of uncertainty in deriving physical quantities from such data, namely i) potential contamination by galactic cirrus, ii) uncertainty in the value of the dust rest-frequency mass-absorption coefficient, iii) difficulty in constraining the dust temperature, and iv) estimation of the appropriate gas:dust ratio in high-redshift objects. Our discussion emphasises how important it will be to quantify and, where possible, minimize such uncertainties (via, for example, appropriate observational strategies) in order to fully capitalize on the ten-fold improvement in sensitivity offered by the imminent arrival of the next generation of bolometer arrays, such as SCUBA on the JCMT.

Taking these uncertainties into account we show that whilst the high-redshift galaxies discussed in this paper are amongst the most dust-rich and luminous objects discovered to date, their far-infrared properties are more comparable with those of the most luminous nearby interacting galaxies than with those expected of primæval giant ellipticals. This conclusion is rather insensitive to the adopted dust temperature, and the appropriateness of our adopted gas:dust ratio is supported by the molecular line detections of lensed objects. Indeed, despite all of the uncertainties peculiar to studying galaxy evolution at sub-millimetre wavelengths, the current uncertainty over the true value of $\Omega_0$ is probably the most important factor affecting our conclusions.

**Key words:** Cosmology, radio galaxies, submillimetre astronomy, galaxy formation, starformation, dust.

## 1 INTRODUCTION

Over the past four years, we have undertaken a number of sub-millimetre observations of high-redshift radio galaxies and quasars (using the single channel $^3$He bolometer UKT14 on the JCMT) aimed at determining the evolutionary status of these objects on the basis of the strength of their rest-frame far-infrared continuum emission. Since the arrival of the new generation of sub-millimetre bolometer arrays is now imminent, this seems an appropriate time to summarize the existing observational results (including our own data presented here), to review the main sources of uncertainty which afflict the meaningful physical interpretation of such data, and, in the light of recent Keck and HST results (Steidel *et al.*1996, Illingworth 1997), to re-appraise the importance of deep sub-millimetre observations for the study of galaxy evolution and formation (Hughes 1996).

The original motivation for attempting to detect sub-millimetre emission in high-redshift galaxies, despite the relative insensitivity of existing sub-millimetre detectors was the realistic possibility that at least some massive galaxies formed the majority of their stars in a relatively short ($< 1$ Gyr) starburst at high redshift, and that the resulting necessarily high star-formation rates ($\simeq 100 \rightarrow 1000 M_{\odot} yr^{-1}$)

could give rise to strong rest-frame far-infrared thermal emission from dust.

This motivation remains as strong as ever despite the recent discovery at *optical* wavelengths of a population of star-forming galaxies at redshifts $z \sim 3$ by Steidel *et al.* (1996). While the space-density of these Lyman-limit galaxies at $z \simeq 3$ indicates that we may be seeing the progenitors of a substantial fraction of present-day bright galaxies, their rather moderate star formation rates ($\sim 10 M_{\odot} yr^{-1}$) would have to be sustained for virtually a Hubble time to produce the most massive elliptical galaxies which exist in the present-day Universe (of stellar mass $\simeq 10^{12} M_{\odot}$). The implication is that, while in the Lyman-limit galaxies we may be seeing the formation of the bulges of spiral galaxies and the cores of some ellipticals (an interpretation supported by their compact spheroidal appearance; Giavalisco *et al.* 1996), certainly for the most massive galaxies the star-formation rates must have been substantially greater ($\geq 100 M_{\odot} yr^{-1}$) at higher redshifts.

Indeed, we now possess rather strong evidence that this must have been the case. First, the basic properties of present-day elliptical galaxies, namely low molecular gas and dust masses, $< 10^8 M_{\odot}$ (Lees *et al.* 1991, Knapp & Patten 1991, Wilkind & Henkel 1995), enormous stellar masses $\sim 10^{11} - 10^{12} M_{\odot}$, determined from the K-band luminosities ($\gg 2 \times L^*$, Taylor *et al.* 1996) of the host galaxies of low-z radio galaxies, RLQs and the most luminous RQQs, and uniform optical-IR colours (Bower, Lucey & Ellis 1992) that are dominated by a well-evolved stellar population, indicate that the bulk of their stars were formed in a relatively short-lived star-burst at high redshift. Second, rather more severe constraints on what the phrase 'high-redshift' must actually mean have been recently provided by Dunlop *et al.* (1996), who have presented spectroscopic evidence that star formation ceased in a $z = 1.55$ radio galaxy at least 3.5 Gyr prior to the epoch at which the galaxy is observed. Such a large age formally excludes an Einstein–de-Sitter cosmology for a Hubble constant $H_0 > 50$ kms$^{-1}$Mpc$^{-1}$ and thus indicates an extreme formation redshift ($z \gtrsim 5$) for this galaxy in almost any cosmological model. This object is not a freak; a second, apparently even older radio galaxy has now been discovered at a similar redshift (Dunlop 1997) and spectroscopy of radio quiet ellipticals in the cluster around the $z = 1.206$ radio galaxy 3C324 indicate similarly old ages for the vast majority of their stellar populations (Dickinson 1997). Third, a radio galaxy has recently been discovered at $z = 4.41$ (Rawlings *et al.* 1996); this demonstrates that at least some massive galaxies were in place at early epochs, and its properties (*e.g.* low rest-frame ultraviolet flux) are not obviously those of a young star-forming system. In summary, despite the important discovery of the star-forming population at $z \simeq 3$ (Steidel *et al.*1996), a growing body of evidence in fact indicates that we have yet to discover the formation epoch of the most massive galaxies and that, given the available cosmological time, the formation of these objects must have been shortlived and hence should be spectacular in at least one wavelength regime.

These last two studies illustrate the key rôle which radio galaxies continue to play in studies of high-redshift galaxy evolution and formation. The main reason for this is that all low-redshift radio galaxies are associated with giant elliptical galaxies (Owen & Laing 1989), and thus it is reasonable to assume that they can be used to trace the evolution of the most massive galaxies back to high redshifts, and early cosmic epochs.

However, while we can be reasonably confident that the hosts of high-redshift radio sources are the progenitors of giant elliptical galaxies, recent years have seen a growing concern that, at least in the most powerful sources, the direct or indirect effects of their active nuclei might stymie any attempt to determine their evolutionary status at optical-infrared wavelengths. For example, the discovery of multi-modal optical structures aligned along the radio axis of high-redshift radio galaxies (Chambers *et al.* 1987; McCarthy *et al.* 1987) seemed at first sight to indicate the assembly of giant elliptical galaxies from the merging of lower-mass clumps at relatively recent redshifts, as expected in certain hierarchical models of structure formation. However, in subsequent years there has been much debate about whether this is true, and about the evolutionary status of high-redshift radio galaxies in general. Early arguments that $z > 2$ radio galaxies contained old evolved stars (*e.g.* Lilly 1988; Lilly 1989) have been questioned (*e.g* Chambers & Charlot 1990; Eales & Rawlings 1993) but there has been a distinct lack of proof that any of the stellar systems are demonstrably young (although arguments have been made that this is the case; *e.g.* 53W002 – Windhorst *et al.* 1991; 0902+34 – Eales *et al.* 1993). The few hints of 'primævality', gleaned from ultraviolet–infrared observations, have remained hard to prove largely because of the way in which high-redshift radio galaxies are typically selected by virtue of their extreme radio luminosity. An inescapable consequence of high radio luminosity appears to be significant non-stellar emission across the ultraviolet, optical and infrared bands (*e.g.* Rawlings & Saunders 1991; Dunlop & Peacock 1993; Eales & Rawlings 1996). In other words huge narrow emission lines, large ultraviolet luminosities and multi-modal structures (which naively one might interpret as evidence for extremely high star-formation rates and dynamically young systems) are now often attributed to to the action of the powerful jets or quasar light emanating from the active nuclei of these extreme objects. On the other hand, even when radio galaxies are faint (*e.g.* the $z = 4.41$ radio galaxy studied by Rawlings *et al.* 1996) it is impossible to disprove huge star-formation rates since, as is the case for some local ultra-luminous IRAS galaxies (Sanders *et al.* 1988), star formation activity may be enshrouded in dust.

This latter point provides the prime motivation for the study described here. A more robust signature of massive star formation than ultraviolet continuum and emission lines is intense FIR emission from dusty, molecular material, where the rate of dust production is proportional to the star formation rate. The dust is heated primarily by the embedded O and B stars which evolve quickly and disperse their surrounding material on similarly short timescales ($\sim 10^7$yrs., Wang 1991). Hence the FIR luminosity provides a measure of the current formation rate (SFR) of massive stars,

$$SFR = \Psi 10^{-10} \frac{L_{FIR}}{L_{\odot}} \quad M_{\odot} yr^{-1} \qquad (1)$$

where $\Psi = 0.8 - 2.1$ (Scoville & Young 1983, Thronson & Telesco 1986). If galaxies at high redshift have FIR luminosities comparable to or greater than low-z ULIRGS

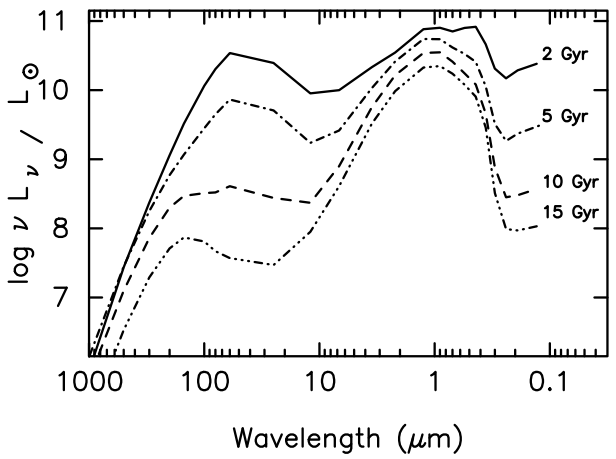


**Figure 1.** The anticipated evolution of the UV to millimetre wavelength rest-frame spectral energy distribution of elliptical galaxies. Models corresponding to galactic ages between 2 - 15 Gyr are shown, assuming a Salpeter IMF with a lower mass limit, $m_l = 0.01M_\odot$. The SFR ($\psi(t) = (m_{gas}/m_{gal})\psi_0$) is proportional to the fractional mass of gas in the galaxy and assumes an intial SFR $\psi_0 = 100M_\odot$/yr. The predicted SEDs are taken from Mazzei, de Zotti & Xu (1994).

($L_{FIR}/L_\odot \geq 10^{12}$), hence SFRs $> 100M_\odot yr^{-1}$, then it is possible that they convert $10^{11} - 10^{12}M_\odot$ of gas into stars in a burst of duration $< 1$ Gyr.

In the Milky Way and local disc galaxies a significant fraction (30%) of the bolometric luminosity ($L_{bol}$) is re-radiated at FIR wavelengths, and hence the SFR (Miller & Scalo 1979, Kennicutt 1983) and the ratio $L_{FIR}/L_{bol}$ cannot have evolved much with look-back time. However the situation is very different for elliptical galaxies. Mazzei, de Zotti & Xu (1994) have modelled the photometric evolution of elliptical galaxies and show that, whilst at the current epoch ellipticals emit $< 1\%$ of their bolometric luminosity at FIR wavelengths, within the first $1-2$ Gyr of their formation this fraction was significantly higher with $L_{FIR}/L_{bol} \sim 0.3$ (see figure 1).

Whilst the details of the evolution are sensitive to the assumed initial mass function (IMF) and SFR, (where the steeper IMF and higher SFR produces a more luminous, but shorter, burst of starformation), it is hard to escape the conclusion that the formation of giant elliptical galaxies is expected to be a spectacular and luminous phenomenon in the rest-frame far-infrared. Indeed this should be true irrespective of whether ellipticals form via the collapse of a single gaseous halo, or grow through the rapid merging of smaller mass clumps at high-z, particularly since the mass dependence of metallicity and mass:light ratio in elliptical galaxies indicates that early star-formation in massive ellipticals should be strongly biassed towards high-mass stars (Zepf & Silk 1996).

Any attempt to detect this thermal radiation from dust in high-redshift radio galaxies would fail were it not for the fact that the expected far-infrared emission peak (at $\lambda \sim 60 - 100\mu m$), due to grains radiating at temperatures of 30–70 K, is shifted into the submillimetre region ($\lambda > 300\mu m$) at the redshifts of interest. Figure 2a demonstrates that, in an Einstein-de Sitter universe and at wavelengths $\geq 800\mu m$, the effects of cosmological dimming on a typical starburst galaxy spectrum are offset between redshifts $z = 1 \rightarrow 10$ by the strongly negative k-correction (which arises as the submillimetre filters effectively climb the Rayleigh-Jeans tail of the thermal dust emission with increasing redshift). The situation for a low density universe is not as advantageous (figure 2b), where the observed flux density for a redshifted object continues to fall, albeit more slowly, in all submillimetre and millimetre wavelength passbands.

In this paper we report on an attempt to exploit the 'detectability' of thermal emission from dust at high redshift to determine the evolutionary status of known high-redshift radio galaxies and quasars. The aim is to use sub-millimetre continuum photometry to estimate or at least constrain the mass of dust in high-redshift objects, with a view to determining both the star formation rate and, more importantly, the mass of gas which has yet to be turned into stars in these potentially young galaxies.

While gas masses can in principle be derived from molecular line observations, we have chosen to concentrate on a sub-millimetre continuum approach for three reasons. First, comparable assumptions and uncertainties also complicate attempts to derive an accurate $H_2$ mass from detections of CO emission. Second, despite determined efforts, with the exception of BR1202−0725 (Omont *et al.* 1996, Ohta *et al.* 1996), no significant detection of molecular gas (through, *e.g.* CO line transitions) has been achieved in any high-z radio-galaxy or quasar (Evans *et al.* 1996, van Ojik *et al.* 1997, Barvainis & Antonucci 1996) unless it has been greatly magnified by gravitational lensing (Barvainis *et al.* 1994, Eisenhardt *et al.* 1996). Third it is in sub-millimetre *continuum* astronomy that the greatest advances in sensitivity are likely to be forthcoming in the immediate future.

As explained above, we have chosen to concentrate on radio galaxies because of their likely association with the high-redshift counterparts of massive elliptical galaxies, but we have also observed a few radio-quiet quasars in an attempt to confirm previously published detections. Our sub-millimetre observations are described in Section 2. In section 3, we present a detailed point-by-point analysis of the various uncertainties which afflict attempts to accurately estimate the dust mass of a high-redshift galaxy from sub-millimetre observations. Then in section 4 we derive our best estimates of the dust masses of these high-redshift objects and use this information to assess their evolutionary status, by estimation of both the star formation rate, and the amount of molecular gas which, at the time of observation, has yet to be converted into stars. Finally, in section 5 we discuss explicitly, and endeavour to quantify the realistic uncertainties in these extrapolations, in particular the gas:dust ratio at high-redshift.

Throughout the paper we assume $q_0 = 0.5$ and $H_0 = 50\mathrm{kms}^{-1}\,\mathrm{Mpc}^{-1}$ unless stated otherwise, and correct previously published data to the same cosmology to allow a comparison of all physical quantities.

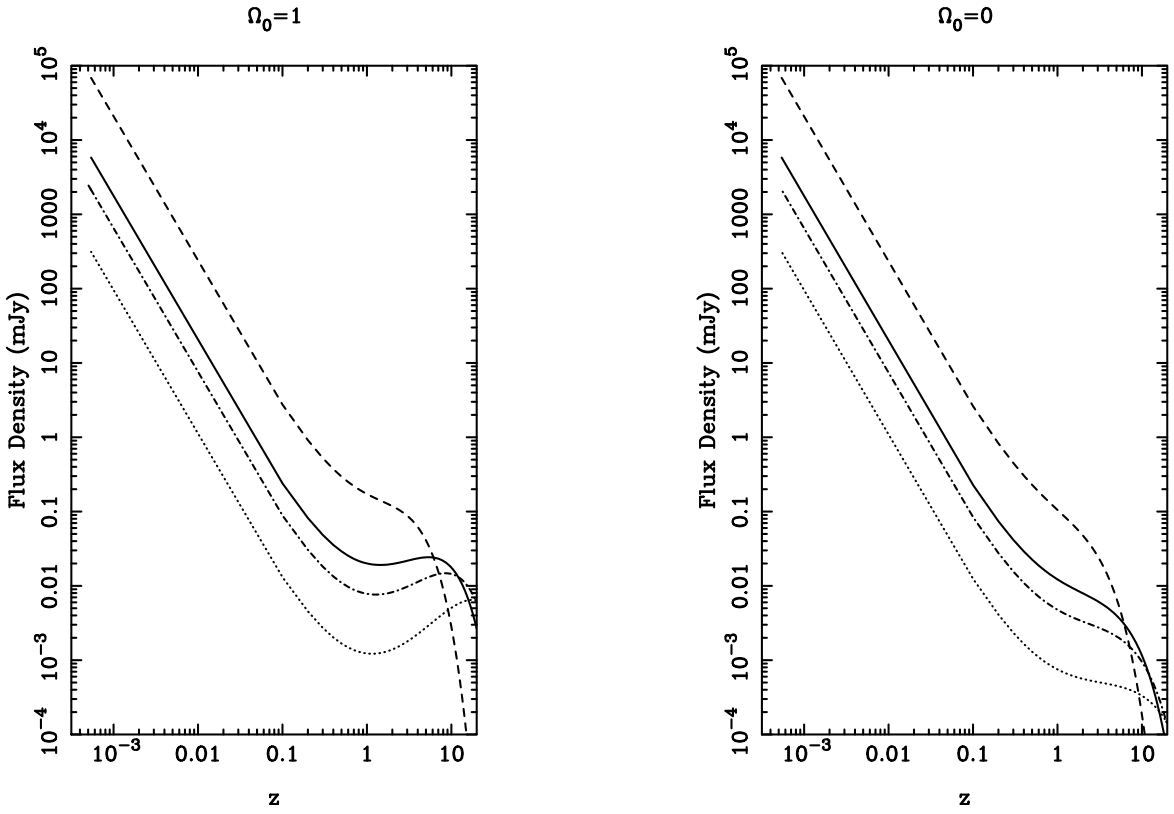


**Figure 2.** Dependence of the observed flux density on redshift of the starburst galaxy M82 (Hughes *et al. 1994*) at 350$\mu m$ (dashed line), 800$\mu m$ (solid line), 1100$\mu m$ (dashed-dotted line) and 2000$\mu m$ (dotted line) for $\Omega_0 = 1$ (left-hand plot) and $\Omega_0 = 0$ (right-hand plot) assuming $H_0 = 50$ km s$^{-1}$ Mpc$^{-1}$.

## 2 SUBMILLIMETRE OBSERVATIONS

### 2.1 Target selection strategy

As figure 2 illustrates, if one wishes to attempt to detect high-redshift ($z > 1$) objects at sub-millimetre wavelengths, little if anything is lost in terms of sensitivity between $z \simeq 1$ and $z \simeq 10$. Consequently, since the star-formation rate in elliptical galaxies is expected to be highest at early times (figure 1) it makes sense to start with the most distant known objects. We thus selected our primary targets (see Table 1) from among the most distant known radio galaxies, concentrating on objects which have been well-studied in the optical-infrared while also attempting to span a meaningful range of radio luminosities and redshifts. 4C41.17 and 8C1435+643 are extremely luminous radio sources and each, at the time they were observed, held the title of the most distant known galaxy in the Universe. B20902+34 is an extremely well-studied object and has been hailed as one of the best known candidates for a primeval galaxy (Eales *et al.* 1993). 6C0032+412 and MG2141+192 are two of the most distant known galaxies at more moderate radio luminosities, while 53W002 is the most distant mJy radio galaxy (Windhorst *et al.* 1991). 3C257 was selected because it is the most distant 3CR radio galaxy and because near-infrared spectroscopy has indicated that Lyman-$\alpha$ emission in this source is attenuated by dust. Two additional radio galaxies at intermediate redshifts ($z \simeq 1$) were selected because of circumstantial evidence suggesting the presence of dust; 3C318 is the most distant radio galaxy detected by IRAS (Heckman *et al.*1994) and 3C65 has an extremely red r–K colour (Lilly 1989, Dunlop & Peacock 1993). Lastly we observed 4 RQQs, again spanning the redshift range ($z = 1 \rightarrow 4$), both to attempt to confirm or refute claimed IRAM detections at millimetre wavelengths, and to enable us to at least make a preliminary attempt to compare the far-infrared properties of radio-loud and radio-quiet objects at high redshift.

### 2.2 Selection of observing wavelength

Obviously we have no *a priori* knowledge of the exact spectral shape of the continuum at FIR-mm wavelengths in the rest frame of the high-redshift radio galaxies. However, since our aim is to test whether these galaxies are undergoing an intense burst of starformation at early epochs, it seems reasonable to assume that their rest-frame FIR-mm continuum spectra will be similar in form to those of massive galactic starforming regions and low-z starburst galaxies. At the highest redshifts the FIR spectral peaks of such starforming regions fall conveniently into the region of two submillimetre wavelength atmospheric windows at 350$\mu m$ and 450$\mu m$ and it might seem that observations would be most profitably made at these wavelengths. However the 750$\mu m$ and 850$\mu m$ atmospheric windows provide more suitable and, in practice, preferential alternatives. At redshifts $z > 2$ the observed flux density ratio $S_{400\mu m}/S_{800\mu m}$ of a starburst galaxy spectrum is significantly smaller than that at $z \sim 0$ (Figure 3) and is no longer sufficient to offset the observational disadvantages of increased sky noise and reduced sky

**Table 1.** 800 $\mu m$ photometry of high-redshift radio galaxies (RGs) and radio-quiet quasars (RQQs). The flux density limits quoted in column 6 are given at the $3\sigma$ level. The references in column 7 give the positions, redshifts and details of other relevant observations.

| Source name | type | $z$ | R.A. (J2000) | Dec (J2000) | $S_{800\mu m}$ (mJy) | refs |
|---|---|---|---|---|---|---|
| 3C 318 | RG | 0.752 | 15 20 05.49 | +20 16 05.1 | <33 | 1 |
| 3C 65 | RG | 1.176 | 02 23 43.48 | +40 00 52.7 | <11 | 1,2 |
| PG1634+706 | RQQ | 1.334 | 16 34 28.97 | +70 31 32.4 | <47 | 3 |
| 53W002 | RG | 2.390 | 17 14 14.78 | +50 15 30.4 | 6.9 ± 2.3 | 4,5 |
| 3C 257 | RG | 2.474 | 11 23 09.40 | +05 30 17.8 | <11 | 6,7,8 |
| H1413+117 | RQQ | 2.546 | 14 15 46.26 | +11 29 43.7 | 66 ± 7 | 9 |
| 2132+0126 | RQQ | 3.194 | 21 35 10.61 | +01 39 31.3 | <12 | 10 |
| B2 0902+34 | RG | 3.391 | 09 05 30.10 | +34 07 57.3 | <14 | 6,11,12 |
| MG 2141+192 | RG | 3.594 | 21 44 07.52 | +19 29 14.2 | <11 | 6,8 |
| 0345+0130 | RQQ | 3.638 | 03 48 02.29 | +01 39 18.4 | <25 | 10 |
| 6C 0032+412 | RG | 3.665 | 00 34 53.09 | +41 31 31.5 | <14 | 8,13 |
| 4C 41.17 | RG | 3.800 | 06 50 52.36 | +41 30 31.5 | 17.4± 3.1 | 14,15,6 |
| 8C1435+643 | RG | 4.252 | 14 36 37.19 | +63 19 14.2 | <13 | 16,17 |

1. Laing *et al.* (1983) 2. Stockton *et al.* (1995) 3. Schmidt & Green (1983) 4. Windhorst *et al.* (1991), 5. Windhorst *et al.* (1994), 6. Eales & Rawlings (1993), 7. McCarthy *et al.*(1995), 8. Eales & Rawlings (1996), 9. Magain *et al.* (1988) 10. Schneider *et al.* (1991) 11. Lilly (1988), 12. Eisenhardt & Dickinson (1992), 13. Rawlings *et al.* in prep, 14. Chambers *et al.* (1990), 15. Miley *et al.* (1992). 16. Lacy *et al.* (1994) 17. Spinrad *et al.* (1995)

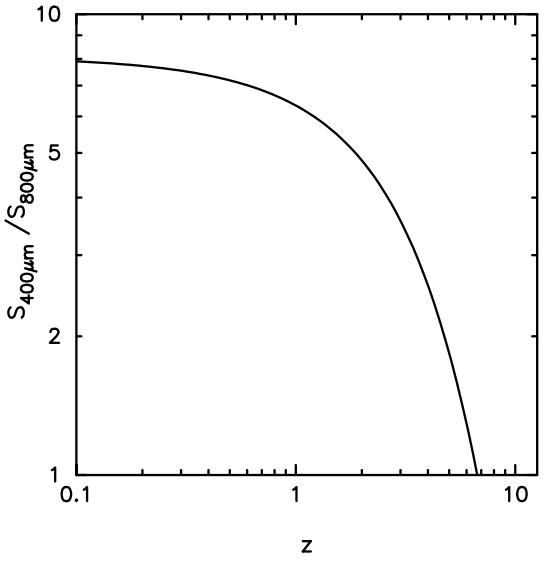


**Figure 3.** The predicted redshift dependence of the observed flux-density ratio $S_{400\mu m}/S_{800\mu m}$ calculated from the isothermal dust model fitted to the FIR-mm continuum data of M82 (Hughes *et al.* 1994).

transparency, $A^{trans}$, at $450\mu m$ compared to $800\mu m$, under even the dryest atmospheric conditions ($p.w.v. \simeq 0.5$ mm) when $A^{trans}(450\mu m/800\mu m)$ is $\leq 0.7$.

Therefore all observations were initally made in the $850\mu m$ and $750\mu m$ windows using a broad-band filter at $\simeq 800\mu m$ ($\lambda_c = 781\mu m$, $\Delta\lambda \sim 200\mu m$). In the event of a detection at $800\mu m$ follow-up observations were made at $450\mu m$. An additional theoretical point also strongly favours the use of a filter at $\sim 800\mu m$ over shorter wavelength filters since, as discussed in §3.3.2, a single photometric measurement at $\lambda \ll 800\mu m$ is virtually useless for constraining the dust masses in sources at $z > 1$.

### 2.3 Observations and Results

Sensitive continuum observations of radio galaxies and RQQs in the redshift range $0.8 \leq z \leq 4.3$ were made at $800\mu m$ using the single-element $^3$He bolometer UKT14 (Duncan *et al.* 1990) on the JCMT during a series of runs between April 1993 and February 1996. Data was taken only under excellent submillimetre observing conditions ($\tau_{800\mu m} \simeq 0.35$). A 65 mm focal-plane aperture was used for all observations and the resulting beamsize of 16.5 arcsec corresponds to physical diameters of $\simeq 140 \rightarrow 100$ kpc at $z = 1 \rightarrow 4$. An azimuthal chop throw of 60 arcsec at a frequency of 7.81 Hz was used to subtract the sky emission. For each source a number of repeated, short (10–20 minute) observations were concatenated using a method described by Hughes *et al.* (1993). Total on-source integration times were typically 3–5 hours. Primary calibration was performed against Uranus and Mars, with secondary calibration against a variety of AGB stars and compact HII regions (Sandell 1994). The data collected to date with UKT14 are summarized in Table 1. Note that, after the successful commissioning of the 0.1K bolometer array SCUBA (> 1997), one can expect typical $3\sigma$ sensitivities of 12 mJy and 1 mJy at $450\mu m$ and $800\mu m$ respectively with an on-source integration of 3 hours.

#### *2.3.1 High-redshift radio galaxies*

A highlight of this study has been the clear detection of 4C41.17 at $800\mu m$, together with a significant upper limit of $3\sigma < 56$mJy at $450\mu m$ (Dunlop *et al.* 1994). This detection was subsequently confirmed by an IRAM observation at 1.25mm (Chini & Krügel 1994) at a level consistent with the thermal dust model presented by Dunlop *et al.*

(1994). We have also achieved a marginal $3\sigma$ detection at $800\mu m$ of 53W002 at a considerably fainter flux density of $6.9 \pm 2.3$ mJy. Yamada *et al.* (1995) have a similarly tentative detection of $^{12}$CO(1–0) in 53W002 leading to an $H_2$ gas mass of $2 \times 10^{12}\,M_\odot$. Whilst we have had no opportunity to confirm our continuum result, treating the $800\mu m$ observation as a limit of $3\sigma \leq 7$ mJy ($M_d = 1.5 \times 10^8 M_\odot$, see §3.2) allows us to place an unlikely lower limit on the gas-to-dust ratio of $> 13000$ and hence casts doubt on the validity of the CO detection. At the time of observation it seemed somewhat surprising that no $800\mu m$ detection of B20902+34 was obtained given the claimed IRAM detection at 1.3 mm (Chini & Krügel 1996). However recent 105 GHz observations (Yun & Scoville 1996, Downes *et al.* 1996) now suggest that a significant fraction (probably the majority) of the 1.3 mm continuum in B20902+34 is due to non-thermal emission (see §3.1). No detections were achieved for the remaining six radio galaxies at z> 2; our non-detection of 8C1435+643 could be regarded as casting some doubt on the validity of the IRAM detection by Ivison (1995), but in fact our 3 sigma upper limit for this source is still just consistent with a grey-body fitted through the 1.25mm data point (see section 3.1).

### *2.3.2 High redshift radio-quiet quasars.*

Continuum observations at $800\mu m$ (Barvainis *et al.* 1992; Isaak *et al.* 1994) and at 1.25 mm (Andreani, La Franca & Cristiani 1993, McMahon *et al.* 1994, Ivison 1995, Omont *et al.* 1996) have suggested that thermal emission from dust has been detected in high-redshift radio-quiet quasars. In an attempt to confirm some of these more marginal results and facilitate direct comparison with our sample of high-redshift radio galaxies, we made $800\mu m$ observations of two (2132+0126 and 0345+0130) of the three radio-quiet quasars detected by Andreani *et al.* (1993). In 2132+0126 the 1.25 mm detection (11.7 mJy) and our measured $800\mu m$ flux density limit (< 12mJy) produce a spectral index $\alpha < 0.06$ ($S_\nu \propto \nu^\alpha$) over the rest-frame wavelength range $298\mu m \rightarrow 191\mu m$. This is inconsistent with that expected from a thermal dust spectrum with a grain temperature $T \geq 20$ K. Therefore our result casts serious doubt either on the 1.25 mm IRAM detections or on the proposed thermal nature of the sub-millimetre continuum, unless the dust grains are significantly colder than observed in low-redshift quasars (Chini *et al.*1989, Hughes *et al.*1993). Our flux limit of $3\sigma < 25$ mJy at $800\mu m$ for 0345+0130 is just consistent with the flux density expected from an extrapolation of the 1.25 mm detection (assuming an isothermal 50 K spectrum with a grain emissivity index $\beta = 2$) and thus provides no additional constraint on the nature of the FIR spectrum or the dust mass in this object.

In the light of the recent detections of the *Cloverleaf* quasar (H1413+117) at 1.25mm, $100\mu m$ and $60\mu m$ (Barvainis *et al.* 1995), which indicated it to have a peculiar SED (figure 4), we dearchived and recalibrated the original submillimetre data of Barvainis *et al.*(1992). Our recalibration at $350\mu m$ and $450\mu m$ agrees with those of Barvainis *et al.*(1992), whilst suggesting a flux density at $800\mu m$ of $66 \pm 12$ mJy, 50% higher than that in the original paper. This prompted us to make a new $800\mu m$ observation of H1413+117 in March 1996 which confirmed our recalibration with a detection of $66 \pm 9$ mJy (R.Ivison & J.Stevens, priv comm.), giving a weighted mean of $66 \pm 7$ mJy for the two independent data sets which differs from the published $800\mu m$ detection of Barvainis *et al.* (1992) at the $2\sigma$ level and is much more consistent with that expected from a greybody fit to the other data-points (figure 4). The SED of the *Cloverleaf* is now one of the most well-defined for a high-z object in the FIR-millimetre wavelength regime and illustrates the difficulty in constraining the dust temperature within the range $30\,K < T_d < 70\,K$ (figure.4, see also §3.3.2).

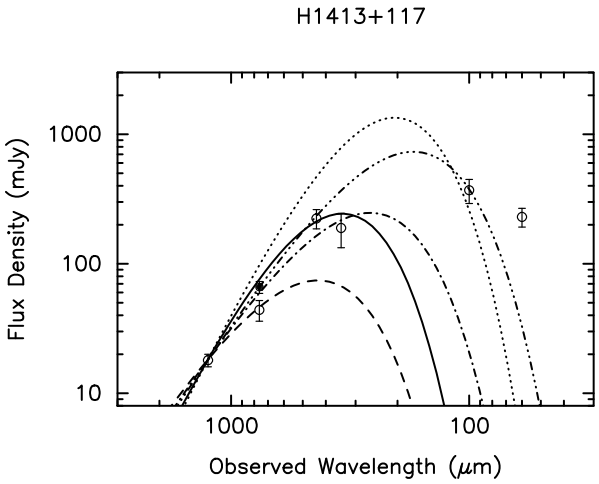


**Figure 4.** The mid-IR to millimetre spectral energy distribution of the *Cloverleaf* quasar (H1413+117). The open circles show the data presented by Barvainis *et al.* (1995). The solid circle shows our new observation at $800\mu m$ that is consistent with various optically-thin isothermal greybody spectra (30 K, $\beta = 2$ - solid curve; 50 K, $\beta = 1$ - dot-dash; 76 K, $\beta = 1$ - dot-dot-dot-dash). Also shown for completeness are greybodies assuming 30 K, $\beta = 1$ (dashed curve) and 50 K, $\beta = 2$ - dotted curve. The alternative greybody spectra are normalised at $1300\mu m$.

## 2.4 Comparison of high-z and low-z AGN at submillimetre wavelengths

In Table 2 we list all galaxies and radio-quiet quasars with redshifts $z > 2$ that have published detections at one or more wavelengths between $350\mu m - 1300\mu m$, regardless of whether they have been confirmed. For the purposes of this paper a '*detection*' is defined as any published photometry with a signal-to-noise ratio $\geq 3$. The reliability of any detection will be discussed when appropriate.

In figure 5 we compare the $800\mu m$ flux densities and limits for the high-redshift galaxies listed in Table 2 with the $800\mu m$ flux densities observed for a variety of starburst galaxies and AGN at low-redshift (Hughes, Davies & Ward 1997). The redshift dependence of the $800\mu m$ flux density of the starburst galaxy M82, previously shown in fig. 2, is reproduced here, together with the dependence for multiples of $\times 10$, $\times 100$ and $\times 1000$ the rest-frame FIR luminosity of M82 ($3 \times 10^{10} L_\odot$). This plot illustrates a number of basic but important points in a rather transparent manner. First, with the exception of IRAS10214+4624 for which, in

this plot, we indicate the inferred $800\mu m$ flux density after correcting for lensing (Eisenhardt *et al.* 1996), there is an obvious absence of sources, at any redshift, with $S_{800\mu m} < 7$ mJy. This simply reflects the current sensitivity limits of sub-millimetre bolometers such as UKT14; it is clear from the figure that our $800\mu m$ observations of the high-z sources are amongst the faintest $800\mu m$ observations made to date. Second, the lines on this plot indicate that for sources at $z > 1$, such flux density limits correspond to FIR luminosities which are several hundred times greater than low-z AGN. Third, this plot shows that with an improvement in sensitivity of a factor of ten (as is promised by new submillimetre bolometer array detectors such as SCUBA on the JCMT) it should be possible to detect objects comparable to the most luminous starburst galaxies and ULIRGS seen in the local universe (*e.g.* Arp220 and Mrk231), with luminosities $L_{FIR} \geq 10^{12} L_{\odot}$ out to $z \simeq 10$. We also note that little effort has been invested in making submillimetre observations of galaxies in the intermediate redshift interval $z = 0.1 \rightarrow 1$.

The important physical property which can be derived directly from these sub-millimetre detections/upper-limits is the mass of dust in a given galaxy. From this one can then go on to assess the evolutionary status of the object in question, either through estimation of the 'current' star-formation rate, or by estimating the gas mass of the object (by adopting a given gas:dust ratio). However, in several recent papers this crucial process has been described with misleading simplicity. In fact, even the first stage in this process (calculating the dust mass) has to be undertaken with great care because there exist at least five potential sources of significant uncertainty. Thus, before attempting to derive the physical properties of the objects listed in Table 2, to assess their evolutionary status (which we do in section 4), in the next section we present a detailed description of these 5 sources of uncertainty, assess their relative importance and outline the prospects for improvements in each area.

## 3 UNCERTAINTIES IN DETERMINING THE DUST MASSES OF HIGH-REDSHIFT OBJECTS

In this section we describe, roughly in order of increasing subtlety, the problems which afflict the accurate determination of dust masses from sub-millimetre observations of high-redshift galaxies. First we consider how one can establish that the detected emission is indeed from dust, rather than being, for example, synchrotron emission (an important issue for our radio galaxy targets). Next we address the issue of how confident one can be that it is the high-redshift target that has been detected, and not merely foreground galactic cirrus. Then, assuming that it can be established that dust emission from the high-redshift target has indeed been detected we consider the effect of uncertainties both in the intrinsic properties of the dust and in its temperature, and discuss what can be done to minimize these uncertainties. Lastly, we briefly highlight the often overlooked implications of the current uncertainty in the values of cosmological parameters.

### 3.1 Potential Problem 1: Have we detected emission from dust?

To prove that any sub-millimetre emission detected from high-redshift galaxies is due to dust one must ideally demonstrate that the sub-millimetre SED is rising too steeply to be due to self-absorbed synchrotron radiation (*e.g.* Chini *et al.* 1989a, Hughes *et al.* 1993). In practice this is extremely difficult to achieve (both due to achievable signal-to-noise, and the fact that at high-redshift one is not always observing the Rayleigh-Jeans tail of the expected thermal emission), but at the very least it is necessary to demonstrate that the observed sub-millimetre spectrum is rising towards shorter wavelengths.

A direct determination of a positive sub-millimetre index $\alpha$ (where $f_{\nu} \propto \nu^{\alpha}$) at high redshift is limited to submillimetre/millimetre continuum observations of only 4 objects; H1413+117 (Barvainis *et al.* 1992, 1995), IRASF10214+4724 (Rowan-Robinson *et al.* 1993), 4C41.17 (Dunlop *et al.* 1994, Chini & Krügel 1994) and BR1202−0725 (Isaak *et al.* 1994, McMahon *et al.* 1994). However, in certain circumstances, even on the basis of a single sub-millimetre or millimetre wavelength, one can be reasonably confident that the detected emission lies above any reasonable extrapolation of the radio emission. This point is well illustrated in Figure 6, in which we present six examples of SEDs from the sources listed in Table 2. The SEDs of 4C41.17, BR1202−0725 and H1413+117 represent good examples of sources whose observed sub-millimetre SED is well determined and for which there can be very little doubt that thermal emission from dust has been detected, whilst the remaining SEDs illustrate the importance but also the limitations of a detection at a single sub-millimetre or millimetre wavelength. For example, our $800\mu m$ detection of 53W002, if real, appears to lie clearly above the extrapolation of its radio spectrum, whereas the millimetre detections of B2 0902+34 (Chini & Krügel 1994) could simply be a detection of the high-frequency tail of the radio emission from the unresolved core (Downes *et al.* 1996) which has a flatter spectrum and is more luminous (with respect to the submillimetre emission) than, for example, the radio-core in the ultra-steep spectrum radio galaxy 4C41.17 (Carilli *et al.* 1994).

Figure 6 demonstrates that with appropriate target selection (*e.g.* ultra-steep spectrum radio sources) and with sensitive sub-millimetre and millimetre photometry one can prove that thermal emission from dust has indeed been detected, but that this must be determined with care on a source-by-source basis. However, even if it can be convincingly demonstrated that the detected emission is due to dust, one must then address the issue of how confident one can be that the dust lies at the redshift of the source. We therefore now address this often over-looked but important issue.

### 3.2 Potential Problem 2: What dust has been detected?: possible contamination by Galactic Cirrus

Even if, as in the case of 4C41.17 and BR1202−0725, it can be shown that a rising sub-millimetre SED has been detected, it must be remembered that extragalactic obser-

**Table 2.** Summary of all published continuum data measuring thermal emission from dust in galaxies at $z > 2$ with at least one detection at wavelengths between $350\mu m$ – 1.25 mm. Flux density limits are quoted at the $3\sigma$ level.

| Source name | $z$ | type | $S_{1.25mm}$ (mJy) | $S_{800\mu m}$ (mJy) | $S_{450\mu m}$ (mJy) | $S_{350\mu m}$ (mJy) | ref. |
|---|---|---|---|---|---|---|---|
| IRAS10214+4724 | 2.286 | IRAS | 24 ± 5 | 50 ± 5 | 273 ± 45 | | 1 |
| 53W002 | 2.390 | RG | | 6.9 ± 2.3 | | | 2 |
| H1413+117 | 2.546 | BALQSO | 18.2 ± 2.0 | 66 ± 7 | 224 ± 38 | 189 ± 56 | 2,3 |
| Q1017+1055 | 3.15 | RQQ | 3.7 ± 1.2 | | | | 4 |
| B2 0902+34 | 3.391 | RG | 3.1 ± 0.6 | < 14 | < 99 | | 2,5 |
| 4C 41.17 | 3.800 | RG | 2.5 ± 0.4 | 17.4 ± 3.1 | < 56 | | 5,6 |
| PC2047+0123 | 3.800 | RQQ | 1.9 ± 0.5 | | | | 7 |
| BR1117−1329 | 3.96 | RQQ | 4.09 ± 0.81 | | | | 4 |
| BR1144−0723 | 4.14 | RQQ | 5.85 ± 1.03 | | | | 4 |
| 8C1435+643 | 4.252 | RG | 2.6 ± 0.4 | < 13 | | | 2,7 |
| BRI1335−0417 | 4.40 | RQQ | 10.26 ± 1.04 | | | | 4 |
| BRI0952−0115 | 4.43 | RQQ | 2.78 ± 0.63 | | | | 4 |
| BR1033−0327 | 4.51 | RQQ | 3.45 ± 0.65 | 12 ± 4 | | | 4,8,9 |
| BR1202−0725 | 4.69 | RQQ | 10.5 ± 1.5 | 50 ± 7 | 92 ± 38 | | 4,8,9 |

1. Rowan-Robinson *et al.* 1993; 2. this paper; 3. Barvainis *et al.* 1995; 4. Omont *et al.* 1996; 5. Dunlop *et al.* 1994; 6. Chini & Krügel 1994; 7. Ivison 1995; 8. Isaak *et al.* 1994; 9. McMahon *et al.* 1994

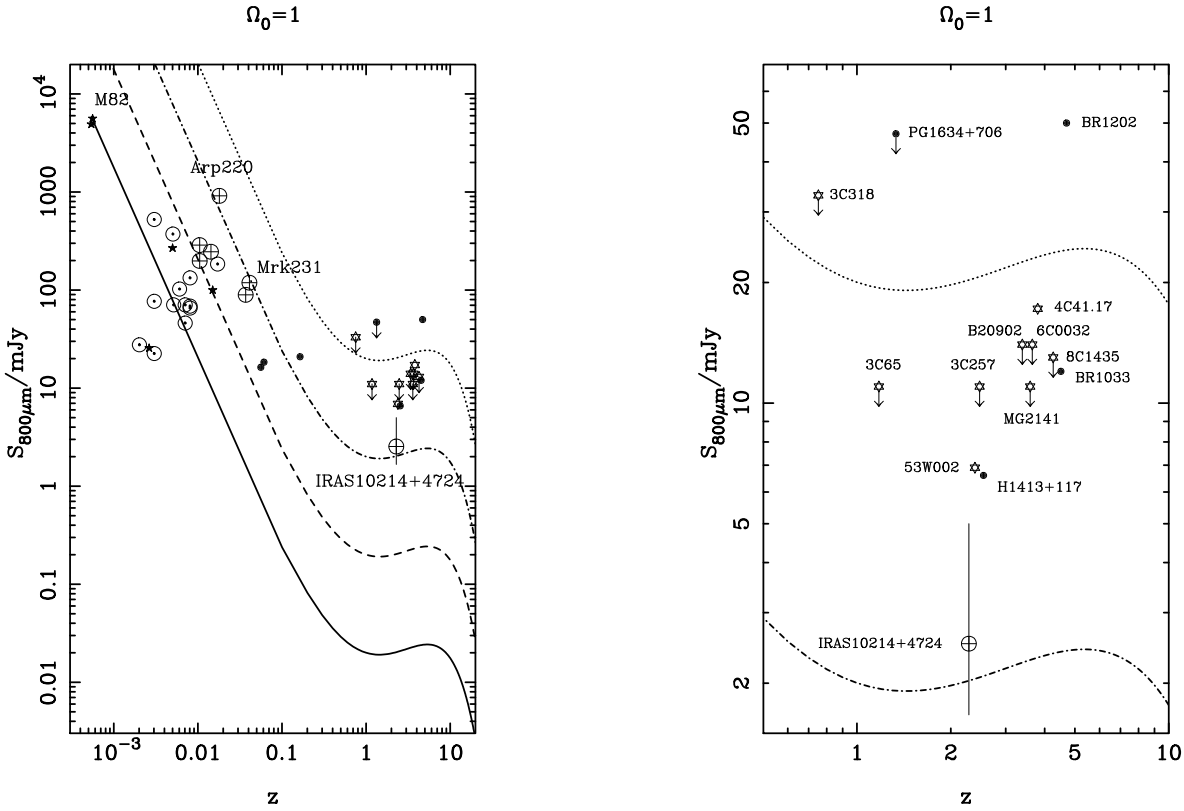


**Figure 5.** A comparison of the measured $800\mu m$ flux densities of various high-z and low-z active galaxies; starbursts (solid-stars), Seyferts (dotted-circles), ULIRGS (crossed-circles), radio galaxies (open-stars), radio-quiet quasars (solid-circles), taken from Hughes, Ward & Davies (1997), Hughes *et al.* (1993) and referenced data included in Table 2 (this paper). The flux densities of IRAS10214+4724 and the Cloverleaf quasar (H1413+117) have been corrected for their amplification due to lensing, see §4. The error-bar associated with IRAS10214+4724 represents the uncertainty in the amplification factor at FIR wavelengths. An expanded version of this figure between redshifts $0.5 \rightarrow 10$ is shown in the right-hand panel. The solid curve represents the predicted dependence of the $800\mu m$ flux density with redshift for the nearby starburst galaxy M82. Also shown are curves for a galaxy with ×10 (dashed), ×100 (dashed-dotted) and ×1000 (dotted) the rest-frame FIR luminosity of M82 ($L_{FIR} = 3 \times 10^{10} L_{\odot}$).

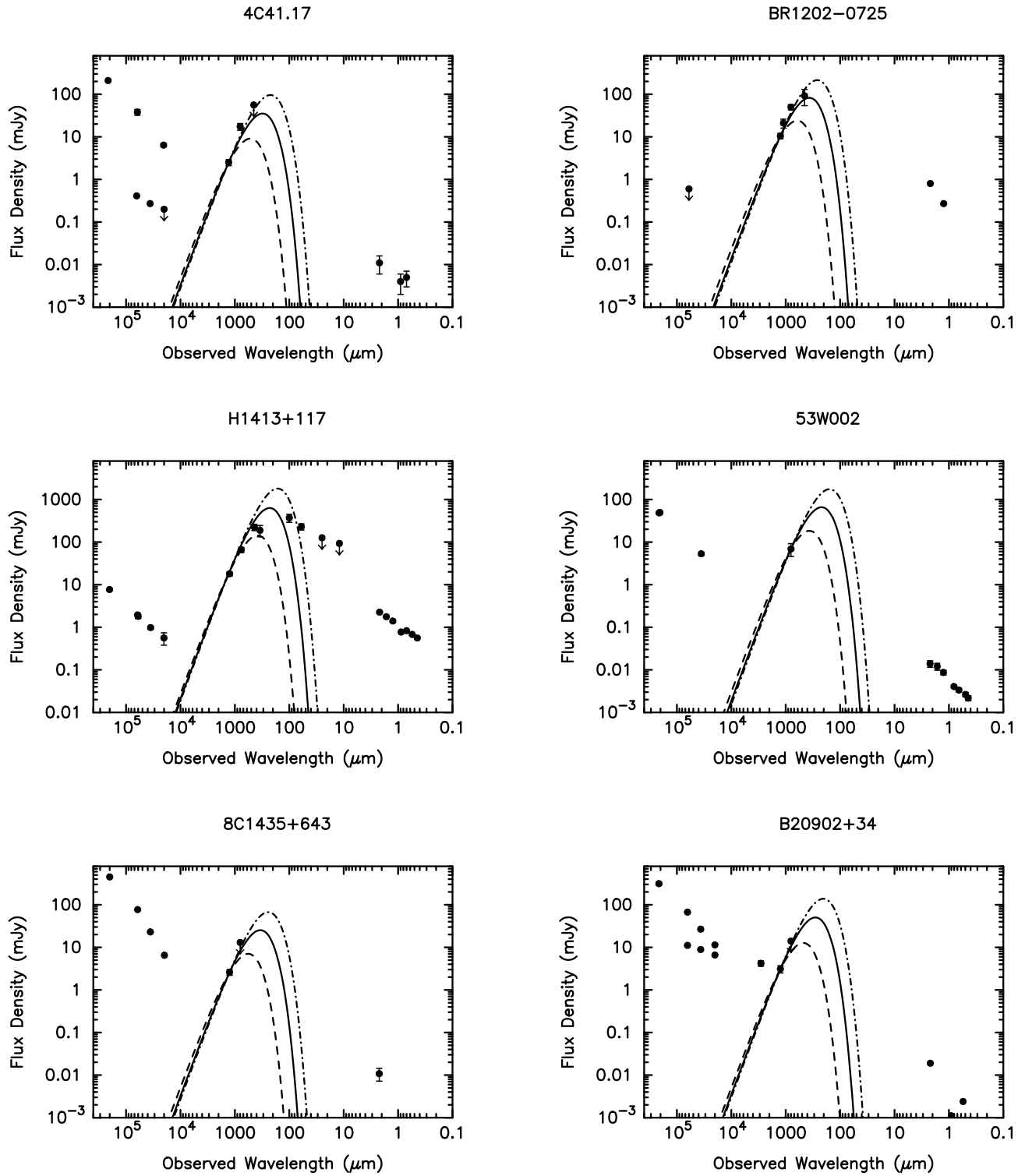


**Figure 6.** Optical-radio SEDs of high-z radio galaxies and radio-quiet quasars showing that, except in the case of B20902+34 (see §3.1), the rest-frame submillimetre and FIR emission is in excess of an extrapolation of the total radio continuum. The SEDs of 4C41.17 and B20902+34 show both the core emission and the steeper large-scale lobe emission. In each case isothermal greybody spectra, assuming an emissivity index $\beta = 1.5$, are shown for 30 K (dashed), 50 K (solid) and 70 K (dotted-dashed). The sub-millimetre and millimetre data are given in Table 2. The radio, infrared and optical continuum fluxes for these objects have been taken from the following papers; 4C41.17 - Carilli *et al.* (1994), Chambers *et al.* (1990: BR1202−0725 - Isaak *et al.* (1994): H1413+117 - Barvainis & Antonucci (1996), Barvainis *et al.* (1995): 53W002 - Windhorst *et al.* (1991): 8C1435+643 - Lacy *et al.* (1994): B20902+34 - Downes *et al.* (1996), Yun & Scoville (1996), Carilli *et al.* (1994), Lilly (1988).

vations at sub-millimetre wavelengths are made in the presence of foreground thermal emission from dust grains in the galactic ISM heated by the interstellar radiation field (Low *et al.* 1984), hereafter *cirrus*. Indeed, given its fractal nature (*e.g.* Bazell & Désert 1988), it is possible that cirrus has significant structure on scales less than the typical $30'' - 60''$ chop-throws employed in submillimetre observations (*e.g.* Meyer 1990, Diamond *et al.* 1989) and hence, since this foreground emission may not be completely removed with the usual technique of position beam-switching, it may represent a significant source of additional noise. In the limit this '*confusion*' noise may place a fundamental constraint on the useful depth of searches for high-z galaxies, and it is therefore important to quantify the contribution of cirrus emission both to the current faint submillimetre observations described in this paper, and to future submillimetre high-redshift surveys.

To achieve this we have reduced the IRAS raw detector data (CRDD) at 12, 25, 60 and $100\mu m$ at the positions of all the high-redshift objects listed in Tables 1 & 2, using the procedure described by Hughes, Appleton & Schombert (1991). Not surprisingly, none of the high-redshift objects were actually detected. The $100\mu m$ surface brightness ($I_{100\mu m}$) of the foreground cirrus was measured towards all of the high-redshift galaxies after the subtraction of any zodiacal emission which can still be significant in the FIR at low ecliptic latitudes.

The average noise level at $100\mu m$ due to cirrus, on scales of a few arcminutes, was $\sim 0.3$MJy/sr which, when extrapolated to $800\mu m$, assuming an isothermal dust spectrum and emissivity index $\beta = 2$ (Rowan-Robinson 1992), gives a brightness of $< 0.3$MJy/sr, equivalent to $< 1$mJy/beam, for cirrus temperatures $> 12$K. In other words it is extremely unlikely that the $800\mu m$ detections, $> 7$ mJy, in Table 2 are due to cirrus unless the dust grains are significantly colder than the generally accepted range of cirrus temperatures, $15K < T < 40K$, (Terebey & Fich 1986, Rowan-Robinson 1986, Van Steenberg & Schull 1988) regardless of grain-size or composition. However, as a caveat we mention firstly that if $\beta \neq 2$, the submillimetre emission can increase by a factor $\sim 10$ as $\beta$ varies between $2 \rightarrow 1$ and, secondly, that the cirrus temperatures are generally derived from a $60\mu m/100\mu m$ intensity ratio which is highly sensitive to the contribution from a small fraction of hot grains in the cloud, and hence the average grain temperature that dominates the mass of the cloud is often over-estimated. At submillimetre wavelengths we are significantly more sensitive to emission from a colder component than in the FIR.

A noise level of $\sim$ 1mJy at $\sim 800\mu m$ is similar to the theoretical predictions of the cirrus confusion on scales equivalent to the chop-throw at submm wavelengths (Helou & Beichman 1991, Gautier, Boulanger, & Puget 1992) assuming that the spatial power spectrum of cirrus, as determined at $100\mu m$ by IRAS (between scales of 8 degs. to 2 arcmins.), continues unbroken to smaller spatial scales ($\sim 30''$), and that the empirical relationship between the amplitude of the variations and the cirrus surface brightness in the FIR is valid at longer sub-millimetre wavelengths.

While these calculations provide reassurance that detections at the level of those described in the present paper are unlikely to be seriously contaminated by cirrus emission, they also demonstrate that cirrus contamination is likely to become a more serious issue with the increased instrumental sensitivity offered from the new generation of submillimetre receivers (*e.g.* SCUBA). With such instruments it will be possible to reach noise levels of $\sim 0.3$mJy/beam or 0.08 MJy/sr in just 3 hours integration and, as a result, future observations of high-redshift galaxies will be sensitive to faint, hence possibly unresolved, clumps of cirrus with temperatures $> 15$K. This result is generalised in figure 7 which shows the surface brightness at $800\mu m$ of galactic cirrus as a function of temperature. The three extrapolated models cover the brightness range of cirrus at $100\mu m$ ($0.1\,MJy/sr < I_{100\mu m} < 10.0\,MJy/sr$) towards the positions of the high-redshift galaxies given in Tables 1 & 2 and are typical of the cirrus background away from the galactic plane ($b > 10^o$) in all but the darkest regions (*e.g.* Lockman *et al.* 1996).

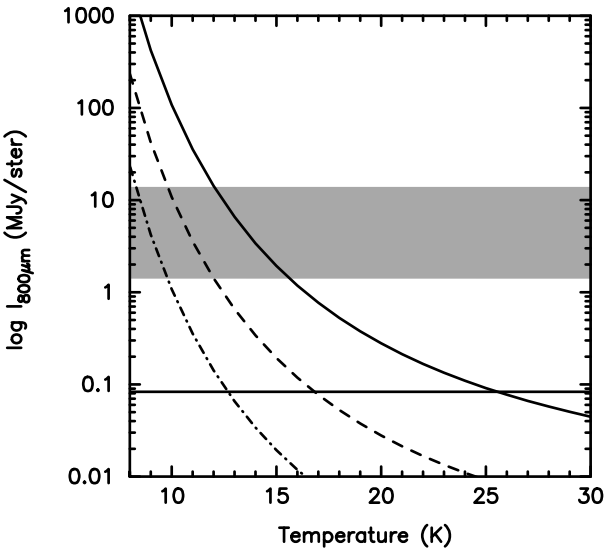


**Figure 7.** Surface brightness at $800\mu m$ of galactic cirrus as a function of dust temperature. The curves are extrapolations of optically-thin, isothermal models with a grain emissivity index $\beta = 2$, assuming a $100\mu m$ intensity of 10 MJy/ster (solid line), 1 MJy/ster (dashed-line), 0.1 MJy/ster (dot-dashed line). The shaded region represents the range of the surface brightness of the $800\mu m$ detections in Table 2 and illustrates that for $T \gg 15$K the contribution from cirrus is negligible. The horizontal line represents the intensity level at $\sim 800\mu m$ that can be reached in 3 hours integration with the future generation of submillimetre receivers, and indicates that deep cosmological studies may suffer from source confusion due to galactic cirrus emission.

### 3.3 Potential Problem 3: Uncertainties in the properties and temperature of the dust grains

If it is assumed the submillimetre continuum ($\lambda_{rest} > 200\mu m$) is due to optically-thin emission from heated dust grains with no additional contribution from bremsstrahlung or synchrotron radiation, a measure of the dust mass $M_d$ can be determined directly from the relationship,

$$M_d = \frac{1}{1+z}\frac{S_{obs}D_L^2}{k_d^{rest}B(\nu^{rest},T)} \quad (2)$$

where $z$ is the redshift of the source, $S_{obs}$ is the observed flux density, $k_d^{rest}$ is the rest-frequency mass absorption coefficient, $B(\nu^{rest},T)$ is the rest-frequency value of the Planck function from dust grains radiating at a temperature $T$, and $D_L$ is the luminosity distance (see section 3.4).

Thus, for a given cosmology and excluding the measurement uncertainty of the continuum flux density, the robustness of dust mass determinations from submillimetre photometry depends on the uncertainty in $k_d$ and $T$. The existing constraints on these two parameters are now briefly discussed in turn.

### *3.3.1 Uncertainty in $k_d(\lambda)$*

Draine (1990) has pointed out that the acknowledged advantage of using optically-thin submillimetre emission to determine the dust mass in galaxies is offset somewhat by increased uncertainty in the properties of interstellar dust, and hence the value of $k_d$ as $\lambda$ is increased from FIR to submillimetre wavelengths. A reasonable estimate of the maximum fractional uncertainty in $k_d$ at $800\mu m$ is $\simeq 7$, with the values of $k_d(800\mu m)$ ranging between 0.04 $m^2$ $kg^{-1}$ (Draine & Lee 1984) and 0.3 $m^2$ $kg^{-1}$ (Mathis & Whifffen 1989) with intermediates values of 0.15 $m^2$ $kg^{-1}$ (Hildebrand 1983) and $0.12 m^2 kg^{-1}$ (Chini, Krugel & Kreysa 1986). In order that we can extrapolate $k_d$ to shorter rest-wavelengths, appropriate for high-z galaxies, we have assumed that $k_d \propto \lambda^{-1.5}$ and have adopted an average value of $k_d(800\mu m) = 0.15 \pm 0.09$ $m^2$ $kg^{-1}$. A different choice of $k_d$ should therefore only be expected to result in dust mass estimates which differ from those which we calculate in section 4, by at most a factor of $\simeq 2$.

### *3.3.2 Uncertainty in T*

The temperature of dust grains that radiate at submillimetre wavelengths and dominate the FIR luminosity in nearby starburst galaxies, low-metallicity dwarf galaxies, ULIRGs, Seyferts and radio-quiet quasars is typically $50 \pm 20$ K (Chini *et al.* 1989a, Chini *et al.* 1989b, Hughes *et al.* 1993, Hughes, Davies & Ward 1997). There is no *a priori* reason to believe that the dust radiating at FIR rest wavelengths in high-redshift radio galaxies and radio-quiet quasars should be significantly different if the star formation processes that exist at early epochs are similar to those in the local universe.

The fractional uncertainty in the dust mass which results from ignorance of the dust temperature within the range $T_1 < T < T_2$ is given by

$$\frac{M_1}{M_2} = \frac{e^{h\nu_{rest}/kT_1}-1}{e^{h\nu_{rest}/kT_2}-1} \quad (3)$$

which increases rapidly as $\nu_{rest}$ moves above the Rayleigh-Jeans tail of the thermal dust emission. Dust mass estimates derived from *rest-frame* sub-millimetre photometry therefore have the benefit of being relatively insensitive to uncertainties in temperature, as compared to dust masses derived from far-infrared data (*i.e.* $\lambda_{rest} < 200\mu m$).

At $z \simeq 0$, where $800\mu m$ photometry samples the Rayleigh-Jeans tail of the thermal dust emission for $T_d \gg 20\,K$, the fractional uncertainty in the estimated dust mass is proportional to the fractional uncertainty in the dust temperature, but as figure 8 illustrates, the uncertainty in $M_{dust}$ increases sharply with increasing redshift unless the observing frequency is reduced appropriately. For example, at $z \simeq 3$ the difference in dust mass between assuming $T = 30\,K$ and $T = 70\,K$ is a factor of 15 and 5 at $450\mu m$ and $800\mu m$ respectively. Consequently our ignorance of the most appropriate value of $T_{dust}$ in high-redshift galaxies is a dominant source of uncertainty in the derived dust masses and it is worth considering the implications of such an uncertainty in future cosmological studies at submillimetre wavelengths.

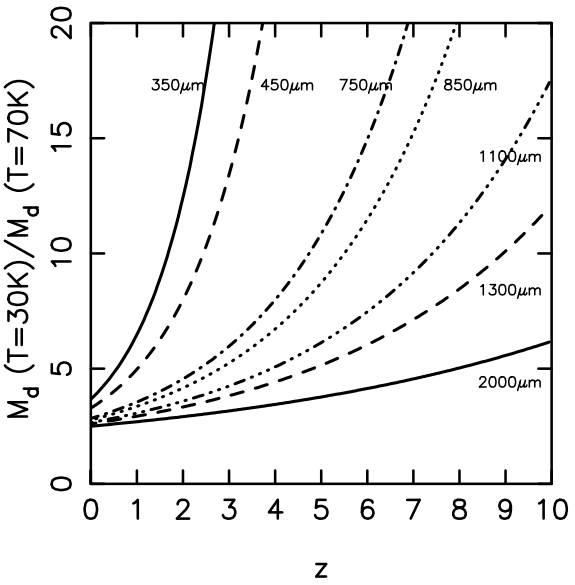


**Figure 8.** Temperature-dependent uncertainty in dust masses deduced from sub-millimetre photometry in various wavebands plotted as a function of source redshift. If we consider a fractional error in dust mass of greater than 5 to be unacceptable, then photometry at $800\mu m$ is of little use for observations of galaxies at $z > 4$, while photometry at $\simeq 400\mu m$ is of little worth (on its own) for $z > 1$.

It is clear that the more one benefits from the increased flux levels offered by intercepting the thermal spectrum nearer the rest-frame $100\mu m$ peak, the greater uncertainty there is in the derived dust mass determined from a single submillimetre continuum measurement. As we have summarised in Table 2, almost all photometric observations at millimetre and submillimetre wavelengths of high-z galaxies have been restricted to filters at $\lambda \geq 800\mu m$, with the exception of IRAS10214+4724, 4C41.17, H1413+117 and BR1202−0725. Thus the majority of data have been made in the rest-frame Rayleigh-Jeans regime (for $T > 30$ K) and consequently, despite the inability of the data to constrain the temperature, the uncertainty in the mass due to this effect alone is no worse than a factor of 5 for galaxies at a redshift $z < 4$.

Figure 8 clearly demonstrates the value of a general philosophy when determining the dust mass from a single photometric detection, that is to use the longest available sub-

millimetre or millimetre wavelength particularly for galaxies at $z > 1$.

### 3.4 Potential Problem 4: Uncertain cosmology

The luminosity distance, $D_L$, which appears in equation 2 is given by

$$D_L = \frac{2c}{H_0\Omega_0^2}\left\{\Omega_0 z + (\Omega_0 - 2)[(\Omega_0 z + 1)^{1/2} - 1]\right\} \quad (4)$$

The (apparently now decreasing) uncertainty in the value of the Hubble constant $H_0$ obviously affects the calculated values of dust mass to some extent, but comparison of the properties of low and high-redshift galaxies is unaffected because $M_{dust}$ simply scales as $H_0^{-2}$.

More serious is our current ignorance of $\Omega_0$. At $z \simeq 4$ if one adopts a low density universe (*i.e.* $\Omega_0 \simeq 0.1$) the derived dust masses are a factor $\simeq 5$ greater than if one assumes an Einstein de-Sitter Universe, and this uncertainty factor rises to $\simeq 15$ at redshifts $z \simeq 10$. The value of pointing out the size of this uncertainty is that it puts into perspective the relatively minor errors which are introduced by our ignorance of the precise value of such parameters as $k_d$.

Bearing these uncertainties in mind, we now proceed to calculate our best estimates of the dust masses of the high-redshift objects listed in Table 2, and hence to infer their evolutionary status.

## 4 DERIVATION OF PHYSICAL PARAMETERS FOR HIGH-REDSHIFT GALAXIES

### 4.1 The dust masses of high-redshift galaxies

At first sight the preceding section may read as a rather depressing litany of ever-increasing sources of error. However, our objective is not to denigrate the usefulness or importance of sub-millimetre cosmology, but rather to delineate and quantify the main sources of error, and to identify what strategies must be adopted to maximise the usefulness of sub-millimetre and millimetre continuum photometry. In fact, for most of the sources listed in Table 2, the current observational constraints indicate that we can still derive realistic and meaningful estimates of their dust masses, with appropriate choices of parameters. First, as illustrated in figure 6, for most of these sources we can be confident that the detected sub-millimetre emission is produced by dust. Second, while it appears that cirrus confusion may be a significant problem for deeper surveys, our estimates of the background cirrus noise for the sources detected here indicate that these detections are unlikely to be significantly effected. Third, we can minimize the effect of disagreement of $k_d$ by choosing an average value. Fourth, for at least some sources (*e.g.* 4C41.17, BR1202−0725, H1413+117) there exists sufficient observational data to set a meaningful upper limit on the dust temperature, and hence lower-limit on the dust mass. Fifth, while it is obviously beyond the scope of this paper to address the issue of the true value of $\Omega_0$, by adopting a high-density universe we can at least ensure that our dust mass estimates are conservative.

We have therefore calculated dust masses for the sources listed in Table 2 using equation 2, assuming $k_d(800\mu m) = 0.15\mathrm{m}^2\mathrm{kg}^{-1}$, $\beta = 1.5$, $T_{dust} = 50$K and $\Omega_0 = 1$. The results are presented in Table 3 and are in the range $1 \times 10^8 - 2 \times 10^9 M_\odot$ allowing for amplifications of order $\sim 11$ (Barvainis *et al.* 1994) and $\sim 10 - 30$ (Eisenhardt *et al.* 1996) for the FIR luminosity in the lensed sources H1413+117 and IRAS10214+4724 respectively.

These dust mass estimates can be used to infer the evolutionary status of the galaxies in two alternative ways. First one can estimate the 'current' star-formation rate of the galaxy. Second one can attempt to estimate the amount of molecular gas in the galaxy which remains to be converted into stars at the epoch of observation. We now consider each of these calculations in turn.

### 4.2 Star formation rates in high-redshift galaxies

As described in the introduction, one can estimate the star-formation rate at the time of observation from their rest-frame FIR luminosities which have been calculated between rest-wavelengths of $2\,mm \rightarrow 10\mu m$ assuming an optically-thin isothermal 50K greybody spectrum (see Table 3), which can be reasonably justified in the case of 4C41.17, BR1202−0725 and H1413+117 (figure 6, see also §4.2.1), normalised to the millimetre and submillimetre flux densities in Table 2. In the absence of any contribution from an AGN or amplification due to lensing, the rest-frame FIR luminosities, which lie in the range $4 \times 10^{12} \rightarrow 6 \times 10^{13}\,\mathrm{L}_\odot$, imply large current SFR's of greater than several $100 M_\odot$/yr. A comparison of the $1000 - 8\mu m$ luminosities of low-z ULIRGs (Sanders *et al.* 1991) with those calculated from a single 50 K isothermal model indicates that we have underestimated the rest-frame FIR luminosities of the high-z galaxies by a factor of $\sim 2.5$ if they contain contributions from hotter dust ($T > 100$K) components which radiate strongly at mid-IR wavelengths. Hence the FIR luminosities and SFRs in Table 3 should be treated as lower-limits when compared to those of lower-redshift galaxies. Further, albeit controversial evidence for extreme SFRs and young galaxy ages ($< 1$ Gyr) have been found in the rest-frame UV-optical morphologies and SEDs of 53W002 and 4C41.17 (Windhorst *et al.* 1991, Chambers *et al.* 1990, Mazzei & de Zotti 1995).

Thus, despite the uncertainties described in §3 we can still conclude that the high-z radio galaxies and radio-quiet quasars, which have been detected at submm-mm wavelengths, are extremely dusty, with dust masses $> 10\times$ larger than observed in their low-z ($z < 0.5$) counterparts (Chini *et al.* 1989a, Knapp & Patten 1991, Hughes *et al.* 1993), and with levels of starformation and starforming efficiencies similar to, or exceeding those observed in low-z ULIRGS (see figure 9).

Particularly if regarded as lower limits, these inferred SFRs are sufficiently high to be at least consistent with the formation of a giant elliptical galaxy in $\simeq 1$ Gyr. However, such a calculation is open to two important criticisms. First, for the active objects considered here it is unclear whether the dust is heated primarily by young stars or by a quasar nucleus, although this argument can be at least partially countered by the fact that the very existence of such large masses of dust indicates extensive recent star-formation. A second, and more important criticism is that an estimate of the 'current' SFR can never shed any light on the length of

**Table 3.** Dust masses, molecular gas masses, FIR luminosities and starformation rates (SFRs) of high-z galaxies. Corrections for the amplification of the FIR emission due to lensing have been applied to the values for IRAS10214+4724 and H1413+117 (see §4.1).

| Source name | $z$ | log $M_d/M_\odot$ | log $M_{H_2}/M_\odot$ | log $L_{FIR}/L_\odot$ | SFR ($M_\odot$/yr) |
|---|---|---|---|---|---|
| 3C318 | 0.752 | $< 9.16$ | $< 11.86$ | $< 13.78$ | $< 6025$ |
| 3C65 | 1.176 | $< 8.72$ | $< 11.42$ | $< 13.35$ | $< 2239$ |
| PG1634+706 | 1.334 | $< 9.35$ | $< 12.04$ | $< 13.97$ | $< 9332$ |
| IRAS10214+4724 | 2.286 | 8.02 | 10.72 | 12.64 | 436 |
| 53W002 | 2.390 | 8.45 | 11.15 | 13.08 | 1202 |
| 3C257 | 2.474 | $< 8.65$ | $< 11.35$ | $< 13.27$ | $< 1862$ |
| H1413+117 | 2.546 | 8.42 | 11.12 | 13.04 | 1096 |
| Q1017+1055 | 3.15 | 8.67 | 11.37 | 13.29 | 1949 |
| B20902+34 | 3.391 | 8.61 | 11.31 | 13.24 | 1738 |
| MG2141+192 | 3.594 | $< 8.58$ | $< 11.28$ | $< 13.20$ | $< 1585$ |
| 6C0032+412 | 3.650 | $< 8.68$ | $< 11.38$ | $< 13.30$ | $< 1995$ |
| 4C41.17 | 3.800 | 8.76 | 11.46 | 13.39 | 2455 |
| PC2047+0123 | 3.800 | 8.36 | 11.06 | 12.99 | 977 |
| BR1117−1329 | 3.96 | 8.62 | 11.32 | 13.24 | 1737 |
| BR1144−0723 | 4.14 | 8.77 | 11.47 | 13.40 | 2511 |
| 8C1435+643 | 4.252 | 8.46 | 11.16 | 13.08 | 1202 |
| BRI1335−0417 | 4.40 | 8.97 | 11.67 | 13.61 | 4074 |
| BRI0952−0115 | 4.43 | 8.43 | 11.13 | 13.05 | 1122 |
| BR1033−0327 | 4.51 | 8.57 | 11.27 | 13.19 | 1549 |
| BR1202−0725 | 4.69 | 9.18 | 11.88 | 13.81 | 6456 |

time over which such a high star-formation rate has been maintained. In other words it is clearly impossible to distinguish a brief, albeit violent burst of star-formation activity (triggered, perhaps, by an interaction) from the sort of sustained high-level star-formation required to produce $\simeq 10^{11} \rightarrow 10^{12} M_\odot$ of stars. What is required is some estimate of the past and future star-formation history of the galaxy. Such an estimate can be provided, to first order, by using the calculated dust mass of a galaxy to estimate its gas mass.

#### *4.2.1 Are simple isothermal models adequate?*

We have assumed that the rest-frame FIR luminosities in table 3 are dominated by radiation from grains with an average temperature of 50K, and that the SFRs can be derived from a single isothermal component. This is of course a simplification, since *real* galaxies clearly have a distribution of grain temperatures that contribute to the rest-frame emission between $200\mu m$ - $50\mu m$. However the thermal emission from grains which radiate at a temperature $T$, with an efficiency $Q_{abs} \propto \nu^\beta$, has a peak in the spectrum of $S_\nu$ at a wavelength $\lambda(\mu m) \sim \frac{5100}{T(K)} \left(\frac{3}{3+\beta}\right)$, and consequently there remains only a restricted range of temperatures (20–70 K) that contribute significantly to the the rest-frame FIR.

In figure 10 we quantify the discrepancy between our calculations of the FIR luminosities in table 3 and, where overlap exists, the bolometric starburst luminosities calculated from the more sophisticated radiative transfer models of Rowan-Robinson (1996) and the evolutionary synthesis models of Mazzei & de Zotti (1996). Figure 10 demonstrates that in the absence of sufficient observational data to constrain models between $800\mu \rightarrow 2\mu$, the adoption of a single average grain temperature (50K) provides extremely good agreement, to within 20%, between the FIR and bolometric luminosities (and also the current SFRs) for galaxies expected to be undergoing vigorous starformation.

### 4.3 Molecular gas masses in high-redshift galaxies

A measure of the total ($HI + H_2$) gas mass of a high-redshift galaxy is a very useful indicator of its evolutionary status because, as long as one can be reasonably confident that the galaxy in question is the progenitor of a present-day giant elliptical (as is the case for radio galaxies), it provides a measure of the fraction of the galaxy which has yet to be turned into stars at the epoch of observation. One way to determine the gas mass of a galaxy is to estimate its molecular ($H_2$) mass from a measurement of the intensity of CO. Unfortunately, in the absence of lensing, it has proved impossible to detect the molecular gas in high-z galaxies directly (van Ojik *et al.* 1997, Evans *et al.* 1996, Barvainis & Antonucci 1996), with the possible exception of BR1202−0725 (Omont *et al.* 1996, Ohta *et al.* 1996). However, an alternative and potentially more productive approach is to convert dust mass to gas mass by adopting a 'reasonable' value for the gas:dust ratio, $M_{H_2}/M_d$. However $M_{H_2}/M_d$ is not a well determined quantity in galaxies in the local universe, let alone at high redshift. Studies of damped Lyman-$\alpha$ systems (DLAAS) currently provide the only opportunity to directly measure the dust content of the universe at early epochs. At $z \sim 3$ it has been suggested that the gas-dust ratio in DLAAS is 400–2000 (Fall, Pei & McMahon 1989, Pettini *et al.* 1994), a value significantly higher than the galactic value of 100–160 (Hildebrand 1983, Savage & Mathis 1979), and on average higher than that found in nearby spirals ($\sim 500$, Devereux & Young 1990), ellipticals ($\sim 700$, Wilkind *et al.* 1995) and ULIRGS ($540 \pm 290$, Sanders *et al.* 1991).

While it may be true that the ratio $M_{H_2}/M_d$ in high-redshift Lyman-$\alpha$ absorbers is significantly greater than in present day galaxies, it seems likely that high-redshift ra-

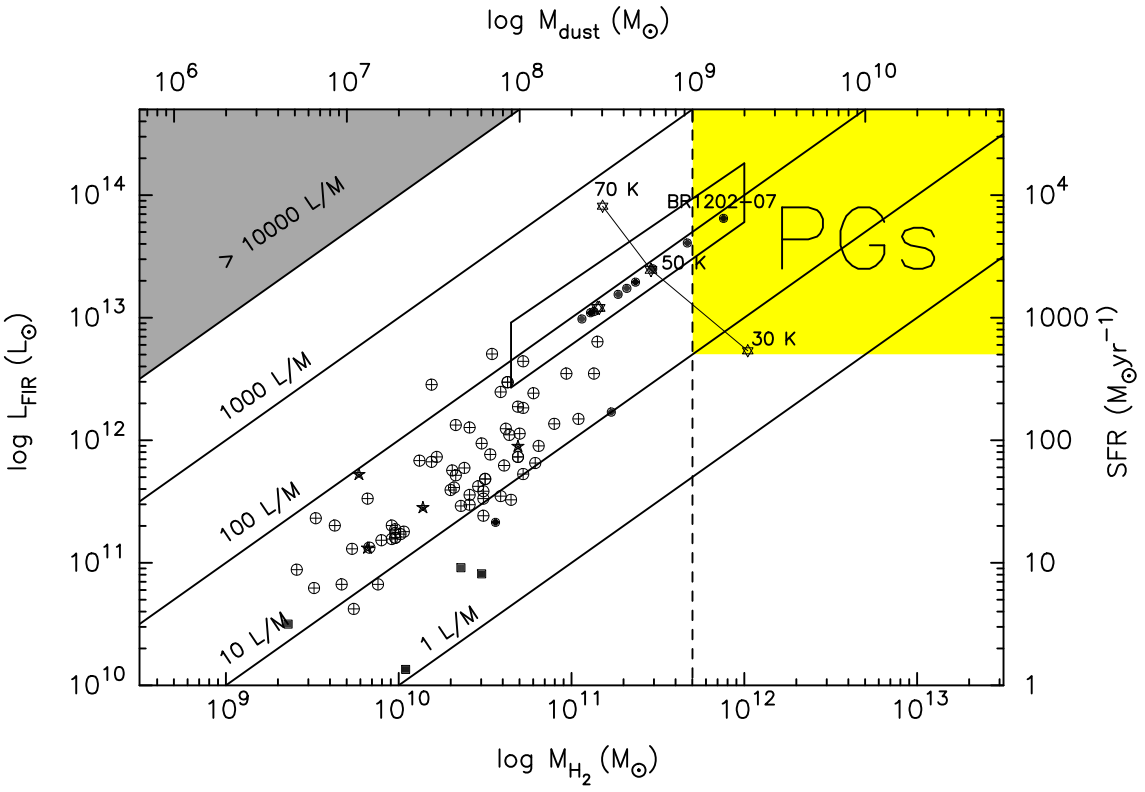


**Figure 9.** A representation of the data given in Table 3 for the detected high-z radio galaxies and radio-quiet quasars, compared to their lower-redshift counterparts, ULIRGs and elliptical galaxies. The symbols have the same meaning as in figure 5, with additional low-z powerful radio galaxies (Mazzarella *et al.* 1993), ULIRGs (Sanders *et al.* 1991) and elliptical galaxies (Lees *et al.* 1991) detected in CO marked as solid stars, crossed-circles and solid squares respectively. The diagonal lines indicate constant $L_{FIR}/M_{H_2}$, while the vertical dashed-line shows the gas mass boundary, to the right of which one can expect to find the projenitors of the most massive elliptical galaxies. The parallelogram encloses the high-z galaxies, which lie along the lower boundary, and depicts the typical range of the increase in their FIR luminosities and SFRs due to a contribution from hotter ($T > 50$K) dust (see §4.2). This figure demonstrates that it is difficult, except possibly in the case of BR1202−0725 (although it may be lensed, see §5), to describe any of the high-z galaxies detected at submm and mm wavelengths as genuinely *primæval*, since they lie outside the shaded region marked "PGs" which represents the parameter space populated by primaeval galaxies, with our definition of $M_{H_2} > 5 \times 10^{11}\,M_\odot$ and a SFR$> 500\,M_\odot$. Varying the assumed dust temperature through a reasonable range ($30K \rightarrow 70\,K$), as illustrated by the representative locus passing through 4C41.17, struggles to change this basic conclusion, except perhaps for 4C41.17 itself.

dio galaxies, being the progenitors of present day ellipticals, are considerably more evolved than Lyman-$\alpha$ absorbers at comparable redshift (which, it has been argued, are the progenitors of present-day disc galaxies). Thus there seems to be no clear justification for adopting an extreme gas:dust ratio and so we have decided to adopt a conservative value of $M_{H_2}/M_d \sim 500$, consistent with the values reported for galaxies in the local universe (the appropriateness of this chosen value is discussed further in the next section).

The resulting values of $M_{H_2}$ determined from continuum measurements are listed in Table 3, and, are $\leq 8 \times 10^{11} M_\odot$. These estimates of the $H_2$ gas mass limits are consistent with the failure to detect large reservoirs of molecular gas directly in various CO transitions (Evans *et al.* 1996; van Ojik *et al.* 1997, Barvainis & Antonucci 1996) a fact which lends some circumstantial support to our adopted gas:dust ratio. Nevertheless, these gas masses are still extremely large and represent a significant fraction of the present day stellar mass of the largest elliptical galaxies. The crucial issue of whether this 'significant fraction' could be sufficiently large to indicate that these objects deserve to be described as 'primæval' is considered below in the final section of this paper.

## 5 CONCLUSIONS: THE EVOLUTIONARY STATUS OF HIGH-REDSHIFT GALAXIES

We have presented sensitive continuum measurements at $800\mu m$ of a sample of high-redshift radio galaxies and quasars. These observations were motivated by the goal of determining their evolutionary status in a relatively model independent manner via a measure of their dust masses, star-formation rates, and molecular gas masses. In addition to our $800\mu m$ data presented here, we have taken the opportunity to gather together all other published millimetre

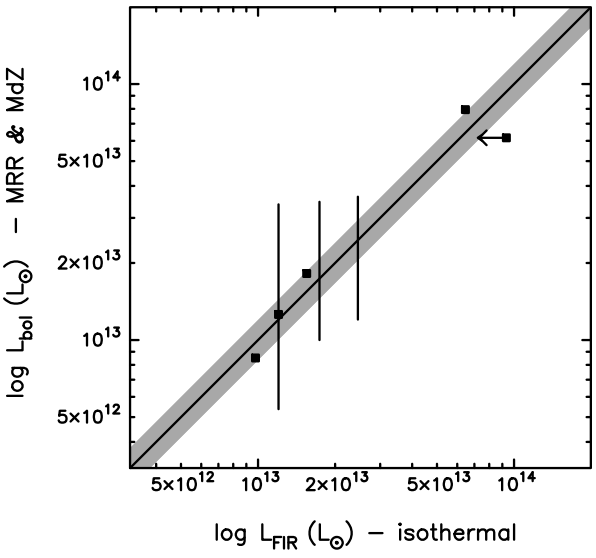


**Figure 10.** A comparison of the rest-frame FIR luminosities ($L_{FIR}$) calculated from a 50K isothermal model (table 3) and the bolometric luminosities ($L_{bol}$) determined from radiative transfer models of Rowan-Robinson (1996, MRR) - filled squares, and from the range of evolutionary synthesis models of Mazzei & de Zotti (1996, MdZ) - lines, which provide a reasonable fit to the submm, optical and IR data. The shaded region represents a maximum discrepancy of 20% about a perfect correlation between the FIR luminosities, and hence SFRs, calculated from isothermal and more sophisticated models.

and submillimetre observations of high-redshift galaxies and quasars at $z > 2$, and Table 3, in effect, summarizes the current status of sub-millimetre cosmology,

While it is expected that this subject will be revolutionized by the significantly more sensitive observations which should be possible in the very near future using new submillimetre continuum bolometer arrays such as SCUBA (Gear & Cunningham 1995), we have argued in this paper that there is much to be learned from considering the uncertainties which afflict the reliable interpretation of the existing, albeit sparse dataset. In this spirit we conclude by considering what can be deduced about the evolutionary status of high-redshift galaxies from the numbers presented in Table 3.

To focus the argument we adopt the strict (and deliberately extreme) definition that a genuinely young elliptical galaxy would be expected to display a very high star-formation rate ($> 500 M_\odot yr^{-1}$), and to contain a total $HI + H_2$ gas mass equivalent to the majority of the stellar mass found in the most massive present-day giant ellipticals (*e.g.* $M_{HI+H_2} \geq 10^{12} M_\odot$). The adoption of such a large present-day mass can be justified on two levels. First, if one wants to unambiguously prove that a given high-redshift object is primæval on the basis of its gas mass, one needs to demonstrate that, even if its eventual present-day stellar mass is extremely large, the bulk of it remains in gaseous form at the high-$z$ epoch of observation. Second, since it is now well-established that the most powerful radio sources and quasars in the low-redshift universe reside in host galaxies with luminosities several times greater than $L^\star$ (Taylor *et al.* 1996), it is not unreasonable to assume that the considerably more luminous active objects listed in Table 3 lie in still deeper potential wells.

Since we are unable to detect the contribution from 21 cm HI emission, which is shifted to 250–500MHz at high-redshift, we use the mean ratio of $M_{HI}/M_{H_2} \sim 1.0 \pm 0.9$ found in elliptical, early-type and interacting galaxies (Lees *et al.* 1991, Young & Knezek 1989), to place a lower mass limit of $M_{H_2} \geq 5 \times 10^{11} M_\odot$ on the molecular gas content of the most luminous primæval or proto-elliptical galaxies.

As illustrated in Figure 9, when judged against these criteria of SFR and $M_{H_2}$, although several of the detected objects in Table 3 may perhaps have adequate star-formation rates, only one source, the quasar BR1202−0725, lies within the parameter space populated by primæval galaxies under the above definition. Given that both IRAS10214+4724 and the Cloverleaf quasar would also have qualified as genuinely young on the basis of the $H_2$ gas mass prior to correcting for the estimated effects of lensing, the suspicion, borne out by the recent CO detection (Omont *et al.* 1996, Ohta *et al.* 1996) must be that BR1202−0725 may also have amplified emission. Therefore based on our analysis, the submillimetre properties of high-redshift AGN, which have been identified at optical/IR/radio wavelengths, are more typical of a strong starburst in an otherwise well-formed galaxy than of genuinely primæval objects. Such a result could indicate that we are seeing the *final* stages of formation of these massive objects, or a starburst triggered by a galaxy-galaxy interaction which is also responsible for the observed AGN activity (in a heirarchical picture of galaxy formation these two alternatives could essentially amount to the same thing).

In judging the robustness of the basic conclusion that these high-z galaxies are *not* primæval, it is important to consider in turn the effect of the dust temperature and adopted gas:dust ratio on the dust masses ($\rightarrow M_{H_2}$) and FIR luminosities ($\rightarrow SFR$) in Table 3 since both of the latter quantities are determined from an isothermal grey-body fit to the submillimetre continuum.

First, the combined effect of the temperature uncertainty ($T_d \sim 50 \pm 20$K) on the FIR luminosities and dust masses, which was discussed at length in §3.3.2, is illustrated in the representative locus passing through 4C41.17 in figure 9. This locus, which is appropriate for galaxies at $z = 2 - 5$ shows that the upper-limit in temperature (70K) moves the high-z sources away from the parameter space occupied by primæval galaxies and into a region requiring extremely high star-forming efficiencies ($\gg 100 L_\odot/M_\odot$). Conversely, while reducing the temperature to 30K can increase the inferred gas mass to close to the required value, this is at the expense of the FIR luminosity and star-formation rate which is reduced to $< 500 M_\odot yr^{-1}$. In summary, our basic conclusion – that we are *not* seeing the primary formation event of these galaxies – is, with the possible exception of 4C41.17, unaffected by varying the temperature of the dust between reasonable limits.

It is worth noting that while our adoption of a dust temperature of 50 K for these high-redshift objects results in values for $L_{FIR}/M_{H_2} \simeq 100$ somewhat greater than is seen in isolated systems at low-redshift ($12 \pm 3 L_\odot/M_\odot$) (Young

*et al.* 1986, Solomon & Sage 1988), such values are not unreasonable and are comparable to that seen in the most luminous low-redshift interacting galaxies ($78 \pm 14 L_{\odot}/M_{\odot}$). Indeed the location of the high-redshift sources on Figure 9 seems perfectly consistent with an extrapolation of the upper envelope of star-forming efficiency defined by the most luminous ULIRGs.

Second, we address the issue of whether the uncertainty in the assumed ratio $M_{H_2}/M_d \sim 500$ (§4.3) can affect our conclusions. Obviously it can if a 'reasonable' range of $M_{H_2}/M_d$ at high-redshift is taken to extend to values of several thousand as suggested by the analysis of Fall *et al.* (1989). However, as already discussed above, the relevance of the investigations of Lyman $\alpha$ absorbers to the present study of high-redshift AGN is dubious. More significant is the good agreement between our adopted value and the mean $M_{H_2}/M_d$ ratio, $(426 \pm 96)$, measured in the only 3 high-z sources (H1413+117, IRAS10214+4724, BR1202−0725) with confirmed CO line and submillimetre continuum detections. The gas:dust ratio in these high-$z$ AGN should be relatively unaffected by lensing assuming that, as in low-$z$ galaxies, the CO and submillimetre continuum have similar spatial distributions, and hence similar amplifications. Thus, taken at face value, these few CO detections of high-redshift objects support our view that $M_{H_2}/M_d \sim 500$ is appropriate for luminous galaxies out to $z \simeq 5$, and explains why sub-millimetre continuum observations of high-redshift objects have been more successful than attempts to detect the molecular gas directly through CO line observations (and casts even more doubt on the claimed CO detection of 53W002, Yamada *et al.* 1995).

To summarize, figure 9 demonstrates that adoption of a dust temperature of 50 K and a gas:dust ratio of 500 leads one to conclude that the high-redshift objects listed in Table 9 would be better described as highly efficient starburst galaxies than genuinely primæval objects. This conclusion is relatively immune to alteration of the adopted dust temperature. Indeed, to alter it significantly requires the adoption of a gas:dust ratio $\simeq 5$ times greater than has been assumed, and the low success rate of molecular CO line observations argues against this option. However, to finish on a cautionary note, there is one way to increase the inferred gas mass without increasing its detectability through line observations, and that is to relax the assumption of an Einstein-de-Sitter Universe. Ignorance of $\Omega_0$ is of course a problem which afflicts studies of galaxy evolution at all wavelengths but, as discussed in section 3.4, at $z \simeq 4$ adoption of $\Omega_0 \simeq 0.1$ instead of $\Omega_0 = 1$ increases the inferred dust mass by a factor of 5 and so, all other things being equal, would increase the values of *both* $L_{FIR}$ and $M_{H_2}$ plotted in Figure 9 by a factor of 5 *for the high-redshift objects only.* Under these circumstances, with star-formation rates ($\simeq 10^3 M_{\odot} yr^{-1}$) and molecular gas masses ($M_{H_2} \simeq 5 \times 10^{11} M_{\odot}$) it would be hard to escape the conclusion that essentially all of the high-redshift objects so far detected at sub-millimetre wavelengths are in fact primæval galaxies (one could, for example, reduce the inferred gas mass by adopting a high dust temperature such as $T \simeq 70$K, but this would in turn imply a truly prodigious star-formation rate).

Thus the unambiguous determination of the evolutionary status of the high-redshift objects detected to date at sub-millimetre wavelengths must await improved constraints on $\Omega_0$. However, we regard it as encouraging for the future of sub-millimetre cosmology that the uncertainties peculiar to the interpretation of these sub-millimetre data can be justified as being comparable in size to the current cosmological uncertainties. In general, continuum observations at sub-millimetre and millimetre wavelengths have proven to be more successful and have provided a comparable or lower $H_2$ mass limit than spectral line data obtained in an equal integration time. This observing efficiency, together with an expected improvement in our understanding of the dust emissivity and gas-to-dust ratio at high-redshift, justifies the continuation of this approach with the future generation of sub-millimetre continuum instruments (*e.g.* SCUBA) which will be sensitive to SFRs $< 100\,\mathrm{M}_{\odot} yr^{-1}$ at $z = 3 - 5$ and hence will detect unlensed versions of IRAS10214+4724 and H1413+117 with ease and also detect the equivalent of low-redshift ULIRGS (*e.g.* Arp220, Mrk231) at $z > 4$. Given that the sub-millimetre properties of the high-redshift radio galaxies and quasars studied to date point towards a more dramatic formation event at yet higher redshift, it will be of particular interest to discover whether any of the objects detected by sub-millimetre surveys meet the criteria defined in Figure 9 for a genuinely primæval giant elliptical galaxy.

## ACKNOWLEDGEMENTS

We are indebted to the referee for helpful comments and suggestions that led to the improvement of this paper. We thank M.S.Yun and N.Z. Scoville for communicating their unpublished 105 GHz measurement of B20902+34. We are also grateful to Jason Stevens and Rob Ivison for confirming our $800\mu m$ observation of H1413+117. The James Clerk Maxwell Telescope is operated by The Observatories on behalf of the Particle Physics and Astronomy Research Council of the United Kingdom, the Netherlands Organisation for Scientific Research, and the National Research Council of Canada. We thank Jeff Cox, Alan Hatakeyama, Ed Lundin, Rusty Luthe, Kimberley Pisciotta and Jim Pomeroy for their valuable assistance at the telescope. DHH gratefully acknowledges receipt of a PPARC PDRA during the course of this work.

## REFERENCES

Andreani P., La Franca F., Cristiani S., 1993, MNRAS, 261, L35
Barvainis R., Antonucci R.R.J., 1996, PASP, 108,187

Barvainis R., Tacconi L., Antonucci R.R.J., Alloin D., Coleman P., 1994, Nat. 371, 586
Barvainis R., Antonucci R.R.J., Colelman P., 1992, ApJ, 399, L19
Barvainis R., Antonucci R.R.J., Hurt T., Colelman P., Reuter H.-P., 1995, ApJ, 451, L9
Bazell D., Désert F.X., 1988, ApJ, 333, 353
Bower R.G., Lucey J.R., Ellis R.S., 1992, MNRAS, 254, 589
Carilli C.L., Owen F.N., Harris D.E., 1994, AJ, 107, 480
Chambers K.C., Charlot S., 1990, ApJ, 348, L1
Chambers K.C. & McCarthy P.J., 1990, ApJ, 354, L9
Chambers K.C., Miley G.K., van Breugel W., 1987, Nat, 329, 604
Chambers K.C., Miley G.K., van Breugel W., 1990, ApJ, 363, 21
Chini R., Krügel E., Kreysa E., 1986, A&A, 167, 315
Chini R., Kreysa E., Biermann P., 1989a, A& A, 219, 87
Chini R., Krügel E., Kreysa E., Gemünd H.-P., 1989b, A&A, 216, L5
Chini R., Krügel E., 1994, A&A, 288, L33
Cimatti A., Freudling W., 1995, A&A, 300, 366
Diamond P.J., Goss W.M., Romney J.D., Booth R.S., Kalberla P.M.W., Mebold U., 1989, ApJ, 347, 302
Devereux N.A., Young J.S., 1990, ApJ, 359, 42
Dickinson M., 1997, In: *HST and the High-Redshift Universe*, eds. N.Tanvir, A.Aragon-Salamanca, J.Wall, World Scientific Press, in press.
Downes D., Solomon P.M., Sanders D.B., Evans A.S., 1996, A&A, 313, 91
Draine B.T., 1990, In: *The Interstellar Medium in Galaxies*, p.483, eds. H.A. Thronson and J.M. Shull, Kluwer, Dordrecht
Draine B.T., Lee H.M., 1984, ApJ, 285, 89
Duncan W.D., Robson E.I., Ade P.A.R., Griffen M.J., Sandell G., 1990, MNRAS, 243,126
Dunlop J.S., 1997, In: *HST and the High-Redshift Universe*, eds. N.Tanvir, A.Aragon-Salamanca, J.Wall, World Scientific Press, in press.
Dunlop J.S., Peacock J.A., 1993, MNRAS, 263, 936
Dunlop J.S., Hughes D.H., Rawlings S., Eales S.A., Ward M.J, 1994, Nat., 370, 347
Dunlop J.S., Peacock J., Spinrad H., Dey A., Jimenez R., Stern D., Windhorst R., 1996, Nat., 381, 581
Eales S.A., Rawlings S., 1993, ApJ, 411, 67
Eales S.A., Rawlings S., 1996, ApJ, 460, 68
Eales S.A., Rawlings S., Puxley P., Rocca-Volmerange B., Kuntz K., 1993, Nat, 363, 140
Eisenhardt P., Dickinson M., 1992, ApJ, 399, L47
Eisenhardt P., Armus L., Hogg D.W., Soifer B.T., Neugebauer G., Werner M.W., 1996, ApJ, 461, 72
Evans A.S., Sanders D.B., Mazzarella J.M., Solomon P.M., Downes D., Kramer C., Radford S.J.E., 1996, ApJ, 457, 658
Fall M.S., Pei Y.C., McMahon R.G., 1989, ApJ, 341, L5
Fukugita, Hogan, Peebles 1996, Nat., 381, 489
Gautier T.N., Boulanger F., Perault M., Puget J.L., 1992, AJ, 103, 1313
Gear W.K., Cunningham C., 1995, In: *Multifeed systems for radio telescopes*, P.A.S.P. Conf Ser., Vol. 75, p.215, eds. D.T.Emerson, J.M.Payne
Giavalisco M., Steidel C.C., Macchetto F.D., 1996, ApJ, 470, 189
Guiderdoni B., Rocca-Volmerange B., 1987, A&A, 186, 1
Heckman T.M., Chambers K.C., Postman M., 1994, ApJ, 391, 39
Helou G., Beichman C.A., 1991, In: *From Ground-Based to Space-Borne Sub-mm Astronomy*, p.117, ESA SP-314
Hildebrand R.H., 1983, QJRAS, 24, 267
Hughes D.H., 1996, In: *Cold Gas at High Redshift*, eds. M.N.Bremer, P.P.van der Werf, H.J.A.Rottgering, C.L.Carilli, Kluwer, p.311
Hughes D.H., Appleton P.N., Schombert, J.M. 1991, ApJ, 370, 176
Hughes D.H., Davies R., Ward M.J., 1997, in preparation
Hughes D.H., Gear W.K., Robson E.I., 1994, MNRAS, 270, 641
Hughes D.H., Robson E.I., Dunlop J.S., Gear W.K., 1993, MNRAS, 263, 607
Illingworth G., 1997, In: *HST and the High-Redshift Universe*, eds. N.Tanvir, A.Aragon-Salamanca, J.Wall, World Scientific Press, in press.
Isaak K., McMahon R., Hills R., Withington, S., 1994, 269, L28
Ivison R.J., 1995, MNRAS, 275, L33
Kennicutt R.C., 1983, ApJ, 272, 54
Knapp G.R., Patten B.M., 1991, AJ, 101, 1609
Lacy *et al.* 1994, MNRAS, 271, 504
Laing, Riley & Longair 1983, MNRAS, 204, 151
Lees J.F., Knapp G.R., Rupen M.P., Phillips T.G., 1991, ApJ, 379, 177
Lilly S.J., 1988, ApJ, 333, 161
Lilly S.J., 1989, ApJ, 340, 77
Lockman F.J., Johoda K., McCammon D., 1996, ApJ, 302, 432
Low F.J. *et al.* 1984, ApJ, 278, L19
Magain P., Surdej J., Swings J., Borgeest U., Kayser R., 1988, Nature, 334, 325
Mathis J.S., Whiffen G., 1989, ApJ, 341, 808
Mazzarella J.M., Graham J.R., Sanders D.B., Djorgovski S., 1993, ApJ, 409, 170
Mazzei P., de Zotti G., 1996, 279, 555
Mazzei P., de Zotti G., Xu C., 1994, ApJ, 422, 81
McCarthy P.J., Spinrad H., van Breugel W., 1995, ApJS, 99, 27
McCarthy P.J., Spinrad H., Djorgovski S., Strauss M.A., van Breugel W., Liebert J., 1987a, ApJ, 319, L39
McCarthy P.J., van Breugel W., Spinrad H., Djorgovski S., 1987b, ApJ, 321, L29
McMahon R.G., Omont A., Bergeron J., Kreysa E., Haslam C.G.T., 1994, MNRAS, 267, L9
Meyer D.M., 1990, ApJ, 364, L5
Miley G.K., Chambers K.C., van Breugel W., Macchetto F., 1992, ApJ, 401, L69
Miller G.E., Scalo J.M., 1979, ApJS, 41, 513
Ohta K., Yamada T., Nakanishi K., Kohno K., Akiyama M., Kawabe R., 1996, Nature, 382, 426
Omont A., Petitjean P., Guilloteau S., McMahon R.G., Solomon P.M., Pecontal E., 1996, Nature, 382, 428
Omont A., McMahon R.G., Cox P., Kreysa E., Bergeron J., Pajot F., Storrie-Lombardi,L.J., 1996, A&A, 315, 1
Owen F.N., Laing R.A., 1989, MNRAS, 238, 357
Pettini M., Smith L.J., Hunstead R.W., King D.L., 1994, ApJ, 426, 79
Rawlings S., Saunders R.D.E., 1991, Nat, 349, 138
Rawlings S., Lacy M.,Blundell K.M., Eales S.A., Bunker

A.J., Garrington S.T.,1996, Nature, 383, 502
Rowan-Robinson M., 1986, MNRAS, 219, 737
Rowan-Robinson M., 1992, MNRAS, 258, 787
Rowan-Robinson M., Efstathiou A., Lawrence A., Oliver S., Taylor A., Broadhurst T.J., McMahon R.G., Benn C.R., Condon J.J., Lonsdale C.J., Hacking P., Conrow T., Saunders W.S., Clements D.L., Ellis R.S., Robson I., 1993, MNRAS, 261, 513
Sandage A. 1972, ApJ, 271, 21
Sanders D.B., Soifer B.T., Elias J.H., Madore B.F., Matthews K., Neugebauer G., Scoville N.Z., 1988, ApJ, 325, 74
Sanders D.B., Scoville N.Z, Soifer B.T., 1991, ApJ, 370, 158
Sandell G., 1994, MNRAS, 271, 75
Savage B.D., Mathis J.S., 1979, Ann. Rev. Astr. Ap., 17, 73
Schmidt M., Green R.F., 1983, ApJ, 269, 352
Schneider D.P., Schmidt M., Gunn J.E., 1991, AJ, 101, 2004
Scoville N.Z., Young J.S., 1983, ApJ, 265, 148
Solomon P.M., Sage L, 1988, ApJ, 334, 613
Spinrad H., Dey A., Graham J.R., 1995, ApJ, 438, L51
Steidel C.C., Giavalisco M., Pettini M., Dickinson M., Adelberger K.L., 1996, ApJ, 462, L17
Stockton A., Kellogg M., Ridgway S.E., 1995, ApJ, 443, 69
Tadhunter C.N., Scarrott S.M., Draper P., Rolph C., 1992, MNRAS, 256, 53p
Taylor G.L., Dunlop J.S., Hughes D.H., Robson E.I., 1996, MNRAS, 283, 930
Terebey S., Fich M., 1986, ApJ, 309, L79
Thronson H., Telesco C., 1986, ApJ, 311, 98
van Ojik R., Röttgering H.J.A., van der Werf P.P., Miley G.K., Carilli C.L., Isaac K., Lacy M., Jenness T., Sleath J., Visser AA., Wink J., 1997, A&A, in press
van Steenberg M.E., Schull J.M., 1988, ApJ, 335, 197
Windhorst R.A., Burstein D., Mathis D.F., Neuschaefer L.W., Bertola F., Buson L.M., Koo D.C., Matthews K., Barthel P.D., Chambers K.C., 1991, ApJ, 380, 362
Windhorst R.A., Gordon J.M., Pascarelle S.M., Schmidtke P.C., Keel W.C., Burkey J.M., Dunlop J.S., 1994, ApJ, 435, 577
Wang B., 1991, ApJ, 374, 456
Wilkind T., Henkel C., 1995, A&A, 297, L71
Yamada T., Ohta K., Tomita A., Takata T., 1995, AJ, 110, 1564
Young J.S., Knezek P.M., 1989, ApJ, 347, L55
Young J.S., Kenny J.D., Tacconi L., Claussen M.J., Huang Y.-L., Tacconi-Garman L., Xie S., Schloerb F.P, 1986, ApJ, 311, L17
Yun M.S., Scoville N.Z., 1996, private communication
Zepf S.E., Silk J., 1996, ApJ, 466, 114